Journal of Medicinal Chemistry

Article

Conjugation of short peptides to dibenzodiazepinone-type muscarinic acetylcholine receptor ligands determines MR selectivity

Andrea Pegoli, David Wifling, Corinna G. Gruber, Xueke She, Harald Hübner, Günther Bernhardt, Peter Gmeiner, and Max Keller

J. Med. Chem., **Just Accepted Manuscript** • DOI: 10.1021/acs.jmedchem.8b01967 • Publication Date (Web): 10 May 2019

ACS Publications

is published by the American Chemical Society. 1155 Sixteenth Street N.W., Washington, DC 20036

Conjugation of short peptides to dibenzodiazepinone-type muscarinic acetylcholine receptor ligands determines M_2R selectivity

Andrea Pegoli,[†,∥,#] *David Wifling,*[†,#] *Corinna G. Gruber,*[†,#] *Xueke She,*[†,§] *Harald Hübner,*[‡] *Günther Bernhardt,*[†] *Peter Gmeiner,*[‡] *and Max Keller**[*,†]

[†]*Institute of Pharmacy, Faculty of Chemistry and Pharmacy, University of Regensburg, Universitätsstr. 31, D-93053 Regensburg, Germany*

[‡]*Department of Chemistry and Pharmacy, Medicinal Chemistry, Friedrich Alexander University, Nikolaus-Fiebiger-Straße 10, D-91058 Erlangen, Germany*

ABSTRACT

Muscarinic acetylcholine receptors (MRs), comprising five subtypes (M_1R-M_5R) in humans, exhibit a high degree of structural similarity. Therefore, subtype-selective MR agonists and antagonists are lacking. We present an approach to highly M_2R-selective MR antagonists based on the conjugation of di- or tripeptides to M_2R-preferring dibenzodiazepinone-type MR antagonists. M_2R selectivity was dependent on the peptide sequence and on the type of linker. The introduction of basic amino acids resulted in improved M_2R selectivity (e.g. UR-AP148 (**48**): pK_i (hM_2R) 8.97, ratio of K_i $M_1R/M_2R/M_3R/M_4R/M_5R$ 49:1:6500:60:400) compared to reported pyridobenzo- and dibenzodiazepinone-type MR ligands. A supposed dualsteric binding mode of the DIBA-peptide conjugates, such as **48**, at MRs was supported by molecular dynamics simulations.

INTRODUCTION

In humans, muscarinic acetylcholine receptors (MRs) comprise five receptor subtypes (M_1-M_5), all belonging to the class A of G-protein coupled receptors. MRs are expressed in the CNS as well as in the periphery being involved in the regulation of, e.g., cognition and smooth muscle contraction, respectively.[1] Due to the high structural similarity of MRs, most pronounced in the region of the orthosteric binding site,[2, 3] subtype-selective MR agonists and antagonists are lacking. Such compounds are considered to improve pharmacotherapy. For example, in the CNS, antagonism at presynaptic M_2Rs has been suggested as an approach to enhance cholinergic function in Alzheimer's disease patients.[4-7] However, for that purpose, highly selective M_2R antagonists are needed, because concomitant blocking of postsynaptic M_1Rs must be strictly prevented.

To date, to the best of our knowledge, only one compound class (diaryl sulfones linked to a piperidinyl moiety) has afforded M_2R ligands with pronounced selectivity (> 100fold in binding affinity) over the other MR subtypes (compound **1a**, Figure 1).[8] Strikingly, the amino group of the anthranoyl moiety in **1a** seems to be crucial for high M_2R selectivity, which becomes obvious from the considerably lower M_2R selectivity of congener **1b**,[8] bearing a methyl instead of the amino group in **1a** (Figure 1). Another well studied class of M_2 subtype-preferring MR antagonists are pyridobenzodiazepinone-type (e.g. **2-4**,[9-12] Figure 1) and dibenzodiazepinone-type (e.g. **5-10**,[10, 13-16] Figure 1) tricyclic MR ligands. The structures and MR binding data of selected tricyclic M_2R antagonists with high M_2R affinity (pK_i > 7.5) (**2-10**), including the most M_2R-selective dibenzodiazepinone-type MR ligand reported in literature to date (**8**),[16] are shown in Figure 1.

Recently, investigations using tritiated analogs of the dibenzodiazepinone-type MR antagonists **7**, **9** and **10**, showing low to moderate M_2R selectivity (Figure 1), revealed that these compounds bind to the M_2R in a dualsteric manner with the tricyclic moiety residing in the orthosteric binding pocket and the 'side chains' reaching the vestibule (common allosteric

site) of the receptor.[15, 16] Moreover, these studies demonstrated that the attachment of various bulky moieties to the dibenzodiazepinone core structure 'A' (*cf*. box in Figure 1) was well tolerated with respect to M_2R binding (e.g. **8-10**).[15, 16]

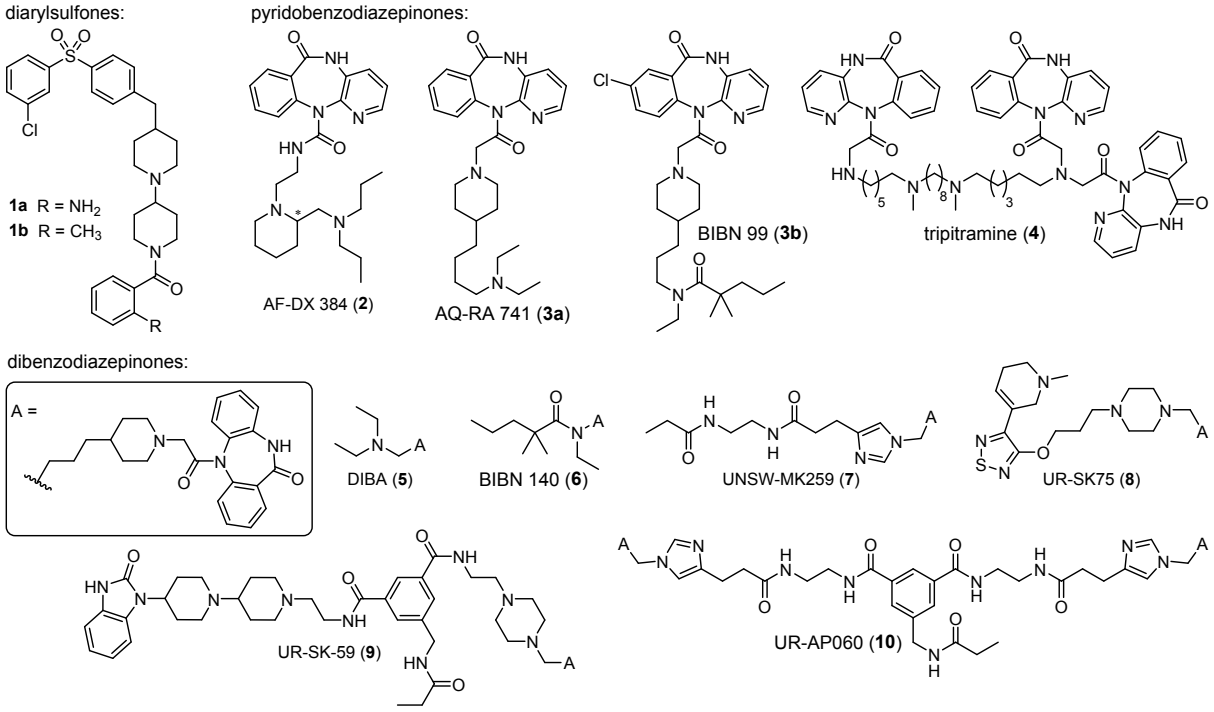

Compd.	Ref.	pK_i M_1	M_2	M_3	M_4	M_5	M_2R selectivity ratios K_i($M_{1,3,4,5}$R)/K_i(M_2R) M_1	M_3	M_4	M_5
1a	a	-	**9.70**	-	-	-	2926	2722	148	186
1b	a	-	**8.57**	-	-	-	230	172	14	48
2, AF-DX 384	b	7.51	**8.22**	7.18	8.00	6.27	5.1	11	1.7	89
	c	7.79	**8.71**	6.75	8.30	6.04	8.3	91	2.6	470
3a, AQ-RA 741	b	7.54	**8.37**	7.20	8.19	6.08	6.8	15	1.5	200
	d	7.3	**8.3**	7.0	8.1	5.9	10	20	1.6	250
3b, BIBN 99	e	5.97	**7.52**	6.11	6.76	5.84	35	26	5.8	48
4, tripitramine	f	8.80	**9.57**	7.42	8.19	7.47	5.9	140	24	130
5, DIBA	g	8.4	**9.5**	8.0	8.7	n.a.	13	37	7.0	-
6, BIBN 140	d	6.5	**8.1**	6.4	7.3	6.5	40	50	6.3	40
7, UNSW-MK259	c	8.07	**9.12**	7.22	8.63	6.75	11	79	3.0	230
8, UR-SK75	h	8.84	**10.1**	7.88	8.59	7.47	20	180	35	470
9, UR-SK59	h	8.56	**9.44**	7.55	8.57	6.96	7.6	78	7.4	300
10, UR-AP060	i	8.82	**9.39**	7.81	9.33	7.64	3.6	37	1.1	55

Figure 1. Structures and MR binding data of two described diarylsulfone-type M_2R-selective MR ligands (**1a**, **1b**) and of a selection of reported M_2R-preferring tricyclic MR antagonists (compounds **2-10**). References: a) Clader *et al*. (reported K_i values (M_2R) were converted to pK_i values; IC_{50}, pIC_{50}, K_i or pK_i values for the MR subtypes M_1, M_3, M_4 and M_5 were not given, instead, only the ratios K_i($M_{1,3,4,5}$R)/K_i(M_2R) were provided),[8] b) Dörje *et al*.,[9] c) Keller

et al. (data reported as pIC_{50}; data were re-analyzed to obtain pK_i values),[14] d) Doods *et al*.,[10] e) Doods *et al*.,[11] f) Maggio *et al*. (reported K_i values were converted to pK_i values),[12] g) Gitler *et al.* (reported K_i values were converted to pK_i values),[13] h) She *et al*.,[16] i) Pegoli *et al.*[15]. Except for **5**, data refer to human receptors. In case of **5**, M_2 and M_4 were rat receptors, whereas M_1 and M_3 receptors were not specified.

As the dualsteric ligand approach is considered useful to develop MR ligands with improved subtype selectivity,[17-20] we wanted to explore, how the attachment of putatively allosterically interacting peptide moieties to the dibenzodiazepinone core structure influences M_2R affinity and selectivity (Figure 2). For this purpose, various di- and tripeptides were conjugated to the dibenzodiazepinone pharmacophore via two linkers, differing in length and polarity, resulting in 'DIBA-peptide conjugates', which were characterized with respect to binding at MRs M_1-M_5.

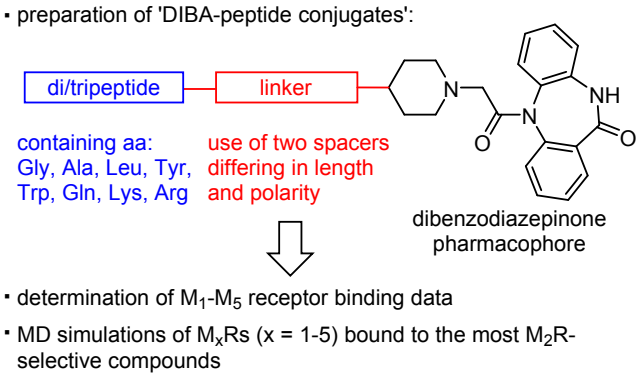

Figure 2. Rationale of the present study.

RESULTS AND DISCUSSION

The selection of amino acids, used to prepare the di- and tripeptide moieties of the DIBA-peptide conjugates, was driven by the fact that acidic amino acids, present at the extracellular surface of MRs, vary in number and position (see Figure S8, Supporting Information).[3, 21, 22]

Therefore, Lys and Arg were chosen as potential interaction partners of these acidic amino acids of the receptor. Gln was used as a non-basic, polar amino acid, capable of forming hydrogen bonds, as well as the aromatic amino acids Tyr and Trp to potentially address Tyr83$^{2.64}$, Tyr177$^{ECL2.51}$ and Trp422$^{7.35}$ located within the vestibule of the M_2R (*cf*. Figure S8A, Supporting Information). Additionally, Ala and Leu were incorporated as nonpolar amino acids. Neither the selection of individual amino acids nor their combination were guided by computational chemistry (docking, simulations) for the following reasons: docking studies alone, requiring considerably less computing time compared to simulations, have limited predictive value; docking studies with subsequent time-consuming simulations were at that stage of the project not considered reasonable to be performed for numerous potential DIBA-peptide conjugates. We rather selected amino acid sequences covering the following combinations of physicochemically different types of amino acid residues: aromatic/aromatic (Trp/Tyr), polar/hydrophobic (Gln/Leu), basic/aromatic (Lys/Tyr) and basic/basic (Lys/Arg or Arg/Arg) (*cf*. Scheme 1). In the tripeptides, Ala was chosen as a 'spacer' amino acid to increase the distance between the aforementioned amino acid pairs.

The estimation of the appropriate length of the linker, by which the dibenzodiazepinone scaffold and the peptide moiety are held together, was supported by the reported crystal structure of the M_2R bound to the non-selective MR antagonist 3-quinuclidinyl benzilate (QNB) (PDB ID: 3UON[21]): recently, induced fit docking of the dibenzodiazepinone derivative **7** (*cf*. Figure 1) to this crystal structure, followed by MD simulation (2 μs), yielded a binding pose of **7** (included in Figure S14, Supporting Information),[15] which was used to identify the putative position of the tricyclic dibenzodiazepinone moiety of the DIBA-peptide conjugates in the orthosteric binding site of the M_2R. The chosen lengths of the two linkers were supposed to allow for a dualsteric binding mode of the DIBA-peptide conjugates, i.e. the dibenzodiazepinone pharmacophore presumably residing in the orthosteric binding site, and the peptide moiety being located in the vestibule or at the surface of the receptor.

The N-terminally acetylated peptides **11-25** were synthesized on a chlorotrityl resin according to the Fmoc strategy. After coupling and Fmoc-deprotection of the final amino acids, the N-termini were acetylated by treatment of the resins with acetic anhydride. The peptides were cleaved off the resin under mild acidic conditions to maintain protecting groups at the side chains (Scheme 1). Coupling of the C-termini of **11-21** to amines **26** and **27**, followed by cleavage of protecting groups, afforded the DIBA-peptide conjugates **28-49** (Scheme 1). Likewise, conjugation of peptides **22-25** to amine **27**, followed by deprotection, yielded compounds **50-53**. Whereas pronounced epimerization occurred during amide bond formation between the peptides and amine **26** or **27** when using HBTU/HOBt as coupling reagent and an excess of DIPEA (data not shown), epimerization was markedly reduced or precluded by using EDC/HOBt as coupling reagent and avoiding excessive DIPEA (in case of amine **26**) or omitting DIPEA (in case of amine **27**). Coupling of Boc-Arg(Pbf)-OH (**54**) to amine **27**, followed by deprotection, afforded **55**, which was acetylated to give **56** (Scheme 1). Propionylation of amine **27** yielded the reference compound **58** (Scheme 1).

Scheme 1. Synthesis of DIBA-peptide conjugates 28-53 and dibenzodiazepinone derivatives 55, 56 and 58.[a]

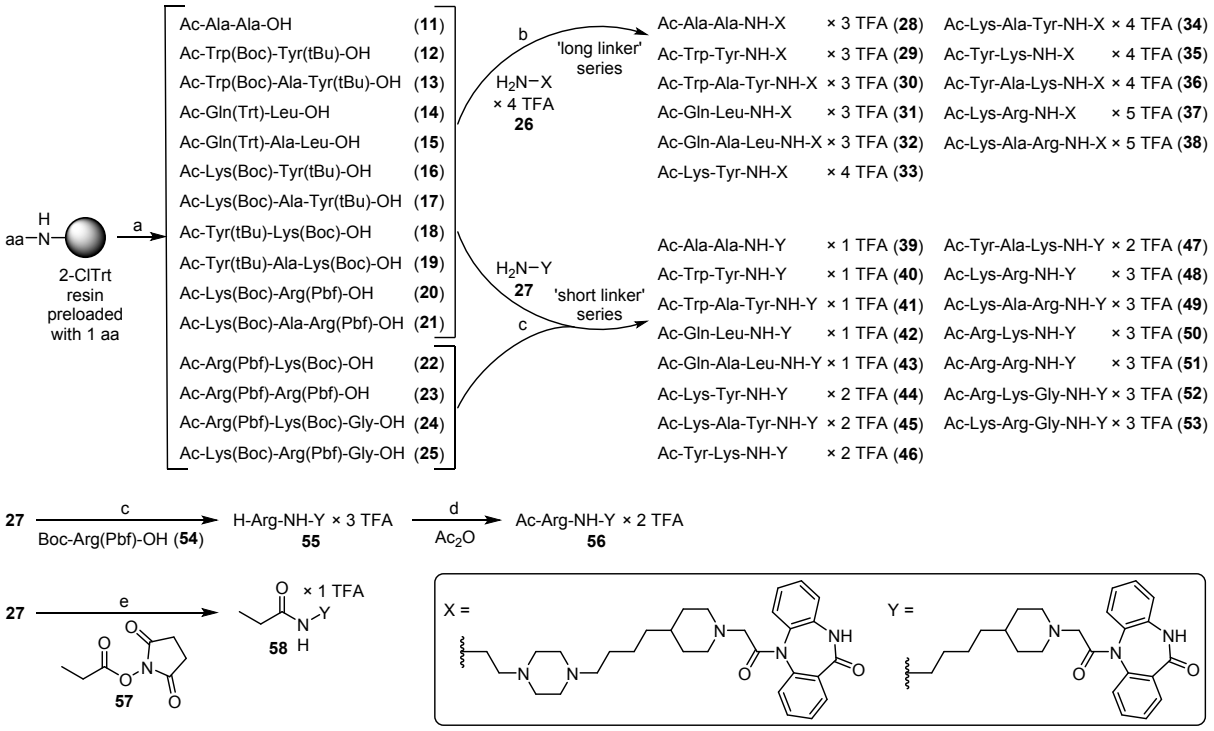

[a]Reagents and conditions: (a) Fmoc-strategy SPPS, amino acid coupling: Fmoc-aa, HBTU, HOBt, DIPEA, DMF/NMP (8:2 v/v), rt or 35 °C, 2 × 60 min ('double coupling'), Fmoc deprotection: 20% piperidine in DMF/NMP (8:2 v/v), rt, 2 × 10 min; (b) (1) EDC, HOBt, DIPEA, DMF, 5 °C, 3 h, (2) TFA/H_2O (95:5 v/v), rt, 3 h, 27-66%; (c) (1) EDC, HOBt, DMF, 5 °C, 3 h, (2) TFA/H_2O (95:5 v/v), rt, 3 h, 30-75%; (d) acetic anhydride, DIPEA, DMF, rt, 2 h, 78%; (e) DIPEA, DMF, rt, 30 min, 80%.

M_1-M_5 receptor affinities of **28-53**, **55**, **56** and **58** were determined by competition binding with the orthosteric MR antagonist [^{3}H]NMS using genetically engineered CHO cells (Table 1) (displacement curves are shown in Figures S1-S5, curve slopes are presented in Table S1, Supporting Information). The subset of compounds with the longer linker, containing a basic piperazine moiety (**28-38**), exhibited higher affinities at all MR subtypes compared to the subset of derivatives containing the shorter linker (**39-53**, **55**, **56**).

Strikingly, within the 'long-linker' subset of compounds (**28-38**), the ranges of pK_i values determined for M_1R, M_2R and M_4R binding were very narrow (pK_i: M_1R 8.50-9.06, M_2R 9.37-10.2, M_4R 8.45-9.04; Table 1). By contrast, the 'short-linker' DIBA-peptide conjugates (**39-53**) exhibited wider ranges of MR affinities (e.g. pK_i M_2R: 6.4-8.97), suggesting that, in case of the M_1, M_2 and M_4 receptor, the SAR of the 'long-linker' series of compounds did not correlate with the SAR of the respective 'short-linker' counterparts. Indeed, this became obvious by plotting the pK_i values (M_1R, M_2R, M_4R) of compounds **28-38** ('long-linker' DIBA-peptide conjugates) against the pK_i values of **39-49** (corresponding 'short-linker' DIBA-peptide conjugates) and linear regression analysis ($R^2 < 0.44$, Figure S6, Supporting Information). Likewise, the SARs of both linker series were also nonparallel in case of the M_3R ($R^2 = 0.061$, Figure S6, Supporting Information). Merely the M_5R binding data revealed a slight linear correlation between the two linker series ($R^2 = 0.71$, Figure S6, Supporting Information). Consequently, the missing correlation between the SARs of the two series of compounds (long *vs*. short linker) is also reflected by disagreeing MR selectivity profiles of individual pairs of compounds differing only in the type of the linker, i.e. bearing identical peptide and dibenzodiazepinone moieties (e.g. **30** *vs*. **41**, selectivity profiles: K_i $M_1R/M_2R/M_3R/M_4R/M_5R$ 27:1:410:19:390 *vs*. 4.7:1:56:1.9:6.2; *cf*. Table 1). The degree of correlation between the selectivity profiles of such pairs of DIBA peptide conjugates became also obvious by plotting the pK_i values (M_1R-M_5R) of the 'short-linker' compound against the pK_i values (M_1R-M_5R) of the 'long-linker' counterpart (Figure S7, Supporting Information): for the compound pairs **29**/**40**, **30**/**41**, **33**/**44**, **35**/**46** and **36**/**47** the correlation was rather low ($R^2 < 0.71$), and for the pairs **28**/**39**, **34**/**45**, **37**/**48** and **38**/**49** a moderate linear correlation was found ($R^2 = 0.83$-0.89).

The DIBA-peptide derivative with the lowest pronounced M_2R selectivity, containing Gln, Ala and Leu, was found in the 'short-linker' subset of compounds (**43**, *cf*. Table 1). The 'long-linker' derivative **38** (UR-AP158) and the 'short-linker' derivative **48** (UR-AP148) exhibited

the highest M_2R affinities within the respective compound subsets as well as higher M_2R selectivities (Table 1) compared to reported, so-called 'M_2R-selective' pyridobenzo- and dibenzodiazepinone-type MR ligands (e.g. **2** and **5**, *cf.* Figure 1).[9-16] As both, **38** and **48**, contain two basic amino acids (Lys, Arg), these results suggest that positively charged residues are advantageous for M_2R binding, being in agreement with reports on orthosteric and allosteric M_2R ligands.[19, 21, 23]

For the majority of the presented compounds, the M_2R selectivity towards the M_1R and M_4R was less pronounced than towards the M_3R and M_5R (Table 1), being consistent with the selectivity profile of previously described, tricyclic M_2R-preferring MR antagonists (*cf.* selectivity profiles of **2**, **3a**, **4** and **7-10** given in Figure 1). The modulatory effect of the peptidyl moiety on M_2R selectivity was confirmed by the low M_2R selectivity of reference compound **58**, which contains a small propionyl group instead of the peptide moiety (Scheme 1, Table 1).

Table 1. M_1-M_5 receptor binding data (pK_i values) of 28-53, 55, 56 and 58 obtained from equilibrium competition binding experiments with [^{3}H]NMS at intact CHO-hM_xR cells (x = 1-5).[a]

cmpd.	structure (for X and Y *cf.* Scheme 1)	pK_i					selectivity toward M_2R (ratios K_i ($M_{1,3,4,5}$R)/K_i (M_2R))			
		M_1R	M_2R	M_3R	M_4R	M_5R	M_1	M_3	M_4	M_5
28	Ac-Ala-Ala-NH-X	8.50 ± 0.05	9.37 ± 0.05	6.81 ± 0.09	8.61 ± 0.10	6.34 ± 0.07	7.5	370	7.5	1100
29	Ac-Trp-Tyr-NH-X	9.06 ± 0.17	9.83 ± 0.12	7.87 ± 0.09	8.97 ± 0.13	7.41 ± 0.04	6.3	79	7.0	220
30	Ac-Trp-Ala-Tyr-NH-X	8.64 ± 0.05	10.1 ± 0.03	7.45 ± 0.06	8.79 ± 0.04	7.51 ± 0.10	27	410	19	390
31	Ac-Gln-Leu-NH-X	8.62 ± 0.04	9.62 ± 0.10	7.21 ± 0.13	8.92 ± 0.15	6.53 ± 0.13	9.6	270	5.4	1300
32	Ac-Gln-Ala-Leu-NH-X	8.53 ± 0.07	9.45 ± 0.05	6.82 ± 0.09	8.45 ± 0.11	6.62 ± 0.10	8.4	440	11	710
33	Ac-Lys-Tyr-NH-X	8.85 ± 0.02	10.1 ± 0.20	7.56 ± 0.01	8.95 ± 0.16	7.15 ± 0.15	14	260	12	780
34	Ac-Lys-Ala-Tyr-NH-X	8.90 ± 0.15	9.76 ± 0.08	7.35 ± 0.07	8.90 ± 0.13	7.02 ± 0.14	8.3	240	8.1	560
35	Ac-Tyr-Lys-NH-X	8.67 ± 0.17	10.1 ± 0.03	7.79 ± 0.06	9.04 ± 0.12	6.85 ± 0.05	32	220	13	1900
36	Ac-Tyr-Ala-Lys-NH-X	8.63 ± 0.10	9.94 ± 0.02	7.55 ± 0.13	8.49 ± 0.03	7.53 ± 0.08	22	290	28	260
37	Ac-Lys-Arg-NH-X	8.91 ± 0.10	10.2 ± 0.06	7.31 ± 0.06	8.69 ± 0.17	6.95 ± 0.11	20	800	37	1900
38 (UR-AP158)	Ac-Lys-Ala-Arg-NH-X	8.64 ± 0.03	10.2 ± 0.03	6.96 ± 0.07	8.68 ± 0.12	6.53 ± 0.09	45	1800	40	4900
39	Ac-Ala-Ala-NH-Y	6.52 ± 0.09	7.64 ± 0.04	5.86 ± 0.03	7.10 ± 0.09	5.87 ± 0.11	14	59	3.7	62
40	Ac-Trp-Tyr-NH-Y	6.81 ± 0.12	7.48 ± 0.05	5.80 ± 0.04	7.03 ± 0.05	7.23 ± 0.12	5.0	46	2.8	1.8
41	Ac-Trp-Ala-Tyr-NH-Y	7.03 ± 0.06	7.70 ± 0.05	5.94 ± 0.04	7.43 ± 0.11	6.92 ± 0.09	4.7	56	1.9	6.2
42	Ac-Gln-Leu-NH-Y	5.98 ± 0.07	6.51 ± 0.02	< 5	5.97 ± 0.08	5.82 ± 0.04	3.4	>27	3.6	4.9
43	Ac-Gln-Ala-Leu-NH-Y	6.27 ± 0.12	6.62 ± 0.10	< 5	6.38 ± 0.11	5.92 ± 0.04	2.2	>36	1.7	4.4
44	Ac-Lys-Tyr-NH-Y	7.52 ± 0.10	8.74 ± 0.08	5.79 ± 0.09	7.97 ± 0.08	7.13 ± 0.12	17	720	5.9	43
45	Ac-Lys-Ala-Tyr-NH-Y	7.23 ± 0.05	8.37 ± 0.02	6.18 ± 0.05	7.63 ± 0.10	6.65 ± 0.05	14	160	5.8	53
46	Ac-Tyr-Lys-NH-Y	7.06 ± 0.01	7.33 ± 0.04	5.00 ± 0.01	6.53 ± 0.08	6.15 ± 0.02	1.8	210	6.6	15

47	Ac-Tyr-Ala-Lys-NH-Y	6.75 ± 0.08	8.03 ± 0.10	5.30 ± 0.04	7.24 ± 0.05	6.68 ± 0.09	19	550	5.9	23
48 (UR-AP148)	Ac-Lys-Arg-NH-Y	7.38 ± 0.14	8.97 ± 0.02	5.17 ± 0.07	7.21 ± 0.06	6.37 ± 0.07	49	6500	60	400
49	Ac-Lys-Ala-Arg-NH-Y	6.94 ± 0.03	8.11 ± 0.02	5.57 ± 0.06	7.05 ± 0.11	6.37 ± 0.08	15	350	12	56
50	Ac-Arg-Lys-NH-Y	7.02 ± 0.08	7.92 ± 0.18	5.26 ± 0.13	6.59 ± 0.06	6.30 ± 0.19	6.5	400	17	39
51	Ac-Arg-Arg-NH-Y	7.70 ± 0.11	8.77 ± 0.03	6.02 ± 0.19	7.53 ± 0.16	6.79 ± 0.05	12	710	19	97
52	Ac-Arg-Lys-Gly-NH-Y	7.64 ± 0.05	8.83 ± 0.10	6.11 ± 0.16	7.76 ± 0.03	6.44 ± 0.13	15	620	11	260
53	Ac-Lys-Arg-Gly-NH-Y	7.49 ± 0.12	8.38 ± 0.05	6.19 ± 0.15	7.56 ± 0.10	6.70 ± 0.10	8.2	180	6.9	49
55	H-Arg-NH-Y	6.97 ± 0.07	8.27 ± 0.12	5.90 ± 0.17	7.25 ± 0.11	5.62 ± 0.11	18	260	9.8	410
56	Ac-Arg-NH-Y	7.01 ± 0.09	7.95 ± 0.09	5.83 ± 0.14	6.83 ± 0.10	6.01 ± 0.11	8.4	140	13	86
58	propanoyl-NH-Y	7.07 ± 0.05	7.10 ± 0.05	5.27 ± 0.08	6.68 ± 0.08	5.15 ± 0.14	1.1	69	2.7	98

[a]Presented are means ± SEM from at least three independent experiments (each performed in triplicate). K_d values (reported previously[14])/concentrations of [^{3}H]NMS: M_1, 0.15/0.2 nM; M_2, 0.090/0.2 nM; M_3, 0.089/0.2 nM; M_4, 0.035/0.1 nM; M_5, 0.24/0.3 nM. The most M_2R selective members of the presented series of compounds are highlighted (**38**, green; **48**, purple).

For **38** and **48**, showing the highest M_2R selectivity, M_2R antagonism was investigated and confirmed in an IP1 accumulation assay[15, 24, 25] (Figure 3). The pIC_{50} values of **38** and **48** amounted to 7.98 and 7.03, respectively. Moreover, plasma stabilities were studied for **38**, **48** and **52**, which proved to be highly stable (> 99% intact compound after 24 h, Table 2).

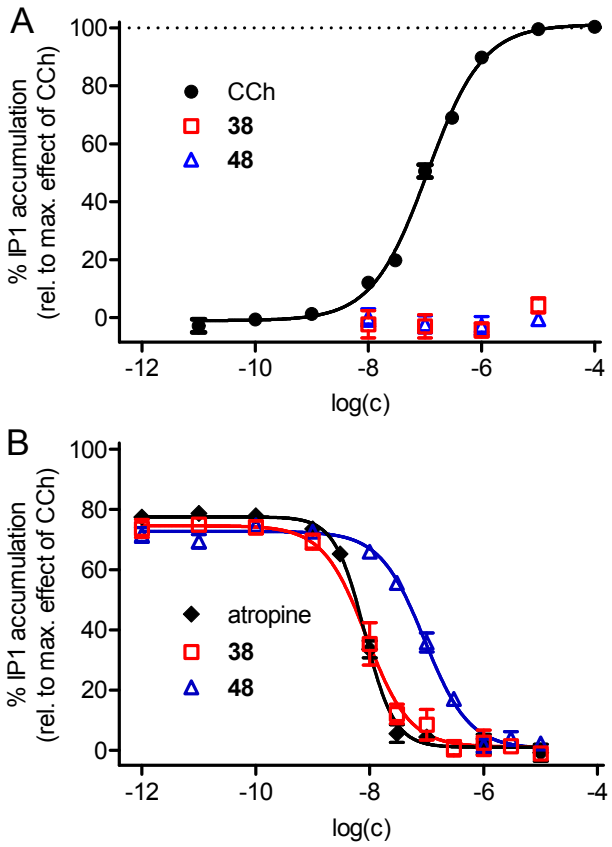

Figure 3. Investigation of M_2R agonism and antagonism of compounds **38** and **48** in an IP1 accumulation assay using HEK-hM_2-G$\alpha_{qi5\text{-}HA}$ cells. (A) Concentration-dependent effects of CCh, **38** and **48** on the accumulation of IP1. **38** and **48** elicited no response. pEC_{50} of CCh (mean ± SEM): 6.97 ± 0.03. Data represent means ± SEM from 14 (CCh) or four (**38**, **48**) independent experiments (performed in duplicate). (B) Concentration-dependent inhibition of the CCh (0.3 µM) induced IP1 accumulation by the MR antagonists atropine, **38** and **48**. pIC_{50} values (means ± SEM): **38**, 7.98 ± 0.19; **48**, 7.03 ± 0.06; atropine, 8.09 ± 0.03. Data represent means ± SEM from four (**38**), five (atropine) or six (**48**) independent experiments (performed in duplicate).

Table 2. Stabilities of **38**, **48** and **52** in human plasma/PBS (1:2 v/v) at 37 °C.[a]

compd.	% intact peptide in plasma after the specified incubation times			
	1 h	6 h	24 h	48 h
38	> 99	> 99	> 99	> 99
48	99 ± 3	> 99	> 99	> 99
52	> 99	> 99	> 99	83 ± 6

[a]The initial concentrations of compounds **38**, **48** and **52** in plasma/PBS (1:2 v/v) were 100 µM. Data represent the mean (± SEM) of three independent experiments (SEM not given when no decomposition was detected). LC-MS analysis revealed the Lys-Gly amide bond in **52** as the major cleavage site (structure of **52** *cf*. Scheme 1 or Table 1).

In order to visualize the interaction of **38** and **48** with MRs by computational chemistry, MD simulations (20 µs) were performed with all MR subtypes bound to **38** or **48** (except for the M_3R bound to **38**). The lowest free energy (MM-PBSA) binding poses obtained from the MD simulations, and the time courses over the simulations are depicted in Figure 4 (M_2R) and Figures S9-S12 (Supporting Information) (M_1R, M_3R-M_5R). The simulations revealed a dualsteric binding mode of **38** and **48** at the M_1R, M_2R, M_4R and M_5R with the tricyclic dibenzodiazepinone moiety residing in the orthosteric binding pocket (Figure 4, Figures S9, S11 and S12, Supporting Information).

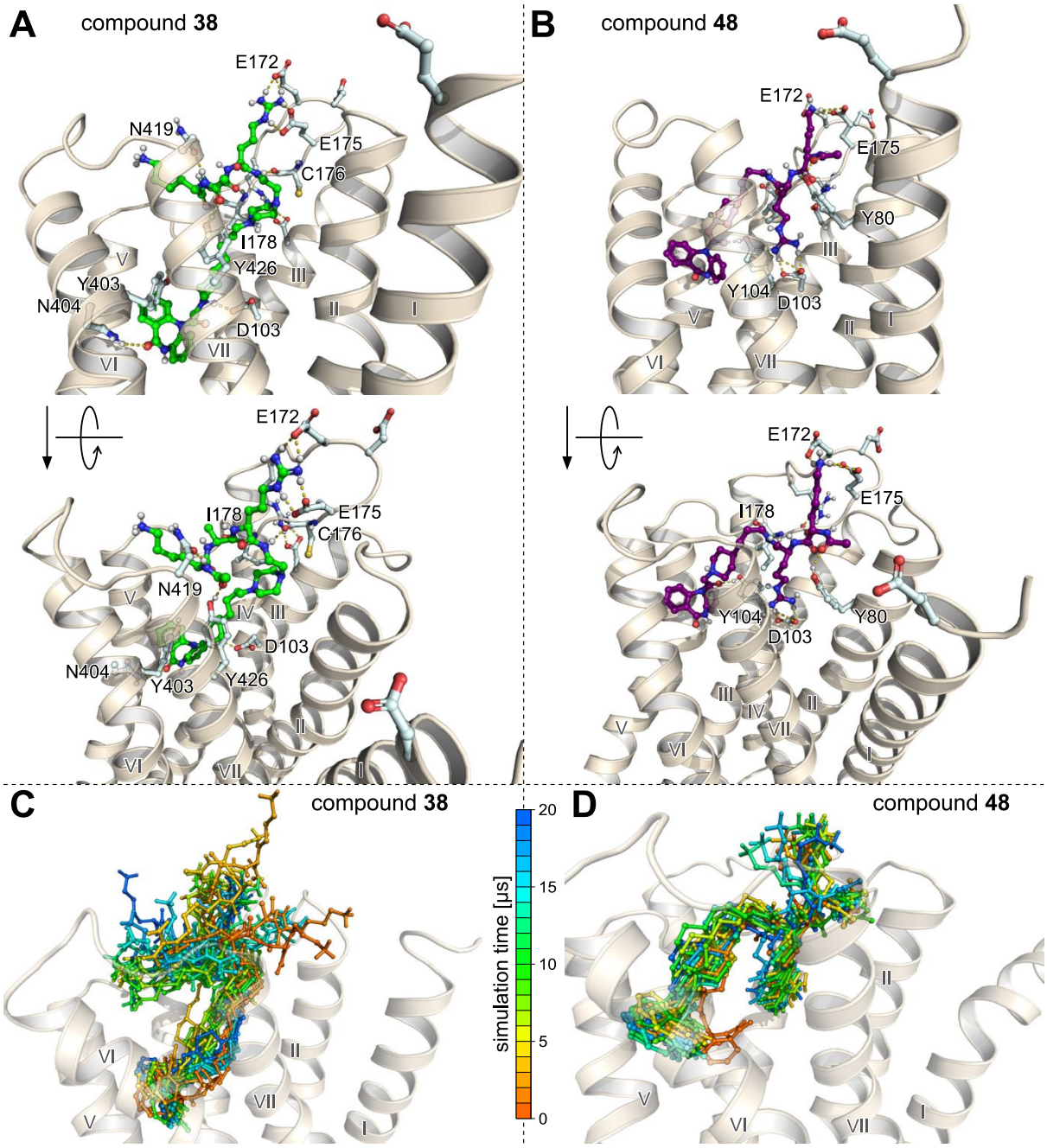

Figure 4. MD simulations (20 µs) of the hM_2R (inactive state, PDB ID: 3UON[21]) bound to **38** (A, C) or **48** (B, D). (A, B) Lowest free energy (MM-PBSA) poses of **38** (green) and **48** (purple), respectively, obtained from analysis of the MD simulation trajectories. Amino acids, involved in H-bonding, salt bridges (both indicated as yellow dashed lines) or π-π interactions (green dashed lines) with the ligands are labeled: in A, $D103^{3.32}$ (HB, SB), $E172^{ECL2}$ (HB, SB), $E175^{ECL2}$ (HB, SB), $C176^{ECL2}$ (HB), $I178^{ECL2}$ (HB), $Y403^{6.51}$ (π-π), $N404^{6.52}$ (HB), $N419^{ECL3}$ (HB) and $Y426^{7.39}$ (HB), in B, $Y80^{2.61}$ (HB), $D103^{3.32}$ (HB, SB), $Y104^{3.33}$ (HB),

E172^{ECL2} (HB, SB), E175^{ECL2} (HB, SB), I178^{ECL2} (HB). (C, D) Time courses of the 20-µs MD simulations of the hM_2R bound to **38** (C) or **48** (D) showing superimposed snap shots collected every 1 µs. HB = hydrogen bond. SB = salt bridge.

This was consistent with previously reported investigations on the binding mode of **7**, **9** and **10** at the M_2R,[15, 16] and in agreement with the fact that **38** and **48** were capable of fully displacing the orthosteric ligand [^{3}H]NMS from M_2Rs when using a high radioligand concentration (i.e. receptor occupancy by [^{3}H]NMS > 95%) (Figure 5), indicating a competitive mechanism between the orthosteric radioligand [^{3}H]NMS and the DIBA-peptide conjugates **38** and **48**. An MD simulation of the M_3R, bound to **38**, was not performed as preceding induced-fit docking afforded no reasonable binding pose for **38**. In case of **48**, the initial dualsteric binding pose of **48** at the M_3R started to disappear during the simulation due to an upward movement of the dibenzodiazepinone moiety ('unbinding' process, *cf*. Figure S10B, Supporting Information), being in agreement with the low binding affinity of **48** at the M_3R (pK_i = 5.17, *cf*. Table 1).

A detailed discussion of the binding modes of **38** and **48**, suggested by MD simulations, is provided in the Supporting Information. It should be mentioned that the coordinates of the recently reported crystal structure of the M_2R in complex with **2** (PDB ID: 5ZKB[26]) were not available at the time the presented MD simulations with the M_2R were performed. As the dibenzodiazepinone substructure of the investigated DIBA-peptide conjugates is structurally similar to compound **2** (structure shown Figure 1), the recently reported M_2R structure[26] might be considered as template for future computational studies of M_2R binding of tricyclic muscarinic receptor antagonists.

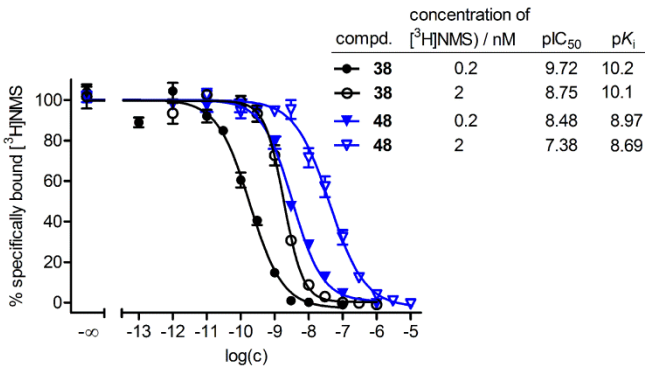

Figure 5. Effect of the DIBA-peptide conjugates **38** and **48** on M_2R equilibrium binding of [^{3}H]NMS (K_d = 0.09 nM) using a radioligand concentration of 0.2 nM (filled symbols, data taken from Figures S2 and S4) or 2 nM (open symbols). Experiments were performed at intact CHO-hM_2R cells at 22 °C. Unspecific binding was determined in the presence of atropine (500-fold excess to [^{3}H]NMS). Data, representing mean values ± SEM from at least four independent experiments (each performed in triplicate), were analyzed by four-parameter logistic fits. The use of a high radioligand concentration, resulting in a high receptor occupancy by [^{3}H]NMS, can 'unmask' a potential non-competitive, negative allosteric mechanism as previously demonstrated, e.g. for the negative allosteric M_2R modulator W84 (indicated by an elevated lower curve plateau and a missing rightward shift of the curves; *cf.* Figure 8C in Pegoli *et al.* 2017[15]). Here, the determination of the effects of **38** and **48** on M_2R equilibrium binding of [^{3}H]NMS yielded curves, which were rightward shifted and exhibited lower curve plateaus not different from zero. This indicates a competitive mechanism between the orthosteric MR antagonist NMS and **38** as well as NMS and **48**.

CONCLUSION

Attachment of di- and tripeptides to dibenzodiazepinone-type MR ligands via two different linkers yielded DIBA-peptide conjugates ('long-linker' series: **28-38**, 'short-linker' series: **39-53**) with medium to high M_2R affinity. M_1R-M_5R binding data of these compounds revealed that M_2R selectivity is dependent on the linker type and can be tuned by the peptide sequence. The study suggests basic residues to be favorable with respect to M_2R selectivity. The following conclusions can be drawn from MR affinities and MD simulations, the latter confirming a dualsteric binding mode at MRs: whereas the longer linker, containing a basic piperazine moiety, is favorable with respect to high M_2R affinity, the shorter aliphatic linker is favorable in terms of tuning MR selectivity by the peptide moiety.

The presented type of selective M_2R antagonists (compounds **38** and **48**) requires, in contrast to M_2R ligands such as **1a** (*cf*. Figure 1), structural optimization with respect to a potential application as therapeutics acting in the CNS. This may be achieved, e.g., by a bioisosteric replacement of strongly basic moieties, such as guanidine groups, by moderately basic surrogates. As MR antagonists such **38** or **48** represent the cold forms of potential tritiated selective M_2R ligands, accessible by replacement of the acetyl residue by a commercially available tritiated acetyl moiety, the presented compound class is superior to **1a** in terms of providing convenient access to radiolabeled M_2R-selective ligands, which represent useful molecular tools.

To the best of our knowledge, the presented approach, i.e. triggering receptor subtype selectivity of small-molecule, nonpeptide receptor ligands by attachment of short peptides, has not been described before. This concept can potentially be applied to other receptor families with respect to the identification of lead structures for the development of dualsteric ligands with improved subtype selectivity.

EXPERIMENTAL SECTION

General experimental conditions. Acetonitrile (HPLC gradient grade) was obtained from Honeywell (Seelze, Germany) or Sigma-Aldrich (Taufkirchen, Germany). DMF, atropine, EDC, DIPEA, HFIP, 1-methyl-D-tryptophan (**59**) and TFA were purchased from Sigma-Aldrich. Absolute EtOH was obtained from Honeywell. CH_2Cl_2, HOBt, DMF for peptide synthesis and NMP for peptide synthesis were obtained from Acros Organics/Fisher Scientific (Nidderau, Germany). Boc-Arg(Pbf)-OH (**54**) was purchased from Carbolution Chemicals (St. Ingbert, Germany). Fmoc-Ala-OH, Fmoc-Arg(Pbf)-OH, Fmoc-Gln-(Trt)-OH, Fmoc-Lys(Boc)-OH, Fmoc-Trp(Boc)-OH, Fmoc-Tyr(tBu)-OH), acetic anhydride and solid supports for SPPS (H-Ala-, H-Arg(Pbf)-, H-Leu-, H-Lys(Boc)-, H-Tyr(tBu)- and H-Gly-2-ClTrt PS resin) were purchased from Merck Chemicals (Darmstadt, Germany). Deuterated solvents were from Deutero (Kastellaun, Germany). HBTU and piperidine were from Iris Biotech (Marktredwitz, Germany). The syntheses of compounds **26**,[16] **27**[14] and **57**[27] were described elsewhere. Millipore water was used for the preparation of buffers and HPLC eluents. 1.5- or 2-mL polypropylene reaction vessels with screw cap (Süd-Laborbedarf, Gauting, Germany) were used for small scale reactions, for the investigation of plasma stabilities and for the preparation and storage of stock solutions. Temperature-controlled reactions and plasma stabilities were performed in 1.5-mL reaction vessels using a Thermocell Mixing Block MB-102 from Bioer (Hangzhou, China). NMR spectra were recorded on a Bruker Avance III HD 600 equipped with a cryogenic probe (14.1 T, ^{1}H: 600.1 MHz, ^{13}C: 150.9 MHz) (Bruker, Karlsruhe, Germany). Abbreviations for the multiplicities of the signals are s (singlet), d (doublet), t (triplet), m (multiplet) and brs (broad-singlet). HRMS was performed on an Agilent 6540 UHD Accurate-Mass Q-TOF LC/MS system (Agilent Technologies, Santa Clara, CA USA) using an ESI source. Optical rotations at 589 nm (Na-D line) were measured on a Polarimeter P8000-T equipped with an electronic Peltier thermostat PT31 (A. KRÜSS Optronic, Hamburg, Germany) using a thermostated (20 °C) micro-cuvette (layer thickness: 1

dm, volume: 0.9 mL) and acetonitrile/water (3:7 v/v) as solvent. Preparative HPLC was performed with a system from Knauer (Berlin, Germany), composed of two K-1800 pumps and a K-2001 detector, or with a Prep 150 LC System from Waters (Eschborn, Germany) consisting of a 2545 Binary Gradient Module, a 2489 UV/Visible Detector and a Waters Fraction Collector III. When using acetonitrile as organic solvent, a Kinetex-XB C18 (5 µm, 250 mm × 21 mm; Phenomenex, Aschaffenburg, Germany) was used as stationary phase at a flow rate of 18 mL/min (**30-33**, **35-38**, **41**, **42**, **44-53**, **55**, **56**) or 20 mL/min (**28**, **29**, **34**, **39**, **40**, **43**, **58**). When using MeOH as organic solvent, a Gemini-NX C18 (5 µm, 250 mm × 21 mm; Phenomenex) served as stationary phase at a flow rate of 15 mL/min (compounds **28** and **39**). Mixtures of 0.1% aq TFA and acetonitrile or mixtures of 0.1% aq TFA and MeOH were used as mobile phase. The detection wavelength was 220 nm. The solvent of collected fractions was removed by lyophilization. Analytical HPLC analysis was performed with a system from Agilent Technologies composed of a 1290 Infinity binary pump equipped with a degasser, a 1290 Infinity autosampler, a 1290 Infinity thermostated column compartment, a 1260 Infinity diode array detector, and a 1260 Infinity fluorescence detector. A Kinetex-XB C18 (2.6 µm, 100 × 3 mm; Phenomenex) was used as stationary phase at a flow rate of 0.5 mL/min (**28-49**) or 0.6 mL/min (**50-53**, **55**, **56**, **58**). Mixtures of 0.04% aq TFA (A) and acetonitrile (B) or A and MeOH (C) were used as mobile phase. The following linear gradients were applied: compounds **28-48**, **50-53**, **55** and **56**: 0-20 min: A/B 90:10-70:30, 20-22 min: 70:30-5:95, 22-26 min: 5:95; compound **58**: 0-12 min: A/B 90:10-70:30, 12-16 min: 70:30-5:95, 16-20 min: 5:95; compounds **28**, **29**, **31**, **32**, **34**, **39**, **42**, **43** and **45**: 0-20 min: A/C 85:15-52:48, 20-23 min: 52:48-5:95, 23-27 min: 5:95; compound **40**: 0-20 min: A/C 85:15-35:65, 20-23 min: 35:65-5:95, 23-27 min: 5:95. For all analytical HPLC runs the oven temperature was set to 25 °C, the injection volume was 20 µL and detection was performed at 220 nm. Compound concentrations were between 40 and 150 µM.

Compound characterization. Target compounds (**28-53**, **55**, **56**, **58**) were characterized by ^{1}H-NMR, ^{13}C-NMR and 2D-NMR (^{1}H-COSY, HSQC, HMBC) spectroscopy, HRMS and RP-HPLC analysis. Additionally, specific optical rotation was determined for compounds **38**, **48** and **52**. The purity (HPLC, 220 nm) of all target compounds amounted to ≥97% (chromatograms shown in the Supporting Information).

Annotation concerning the ^{1}H- and ^{13}C-NMR spectra of **28-53**, **55**, **56**, **58**: due to a slow rotation about the exocyclic dibenzodiazepinone amide group on the NMR time scale, two isomers (ratios provided in the experimental protocols) were evident in the ^{1}H- and ^{13}C-NMR spectra.

Annotation concerning the ^{1}H-NMR spectra (solvent: DMSO-d_6) of **50-53**, **55** and **56**: in order to integrate signals interfering with the broad water signal at ca 3.5 ppm, spectra were additionally recorded in DMSO-d_6/D_2O (4:1 v/v) (spectra shown in the Supporting Information).

Screening for pan-assay interference compounds (PAINS). Screening of all target compounds (**28-53**, **55**, **56**, **58**) for PAINS via the public tool http://zinc15.docking.org/patterns/home[28] gave no hits.

Solid-phase peptide synthesis (Fmoc strategy) of N-terminally acetylated, side chain-protected peptides 11-25. 5-mL BD Discardit II syringes (Becton Dickinson, Heidelberg, Germany) or 5-mL B.Braun syringes (ALMO-Erzeugnisse Erwin Busch, Bad Arolsen, Germany) equipped with a polyethylene frit (average pore size 35 µm; Roland Vetter Laborbedarf, Ammerbuch, Germany) were used as reaction vessels. DMF/NMP (8:2 v/v) was used as solvent throughout (ca 2.2 mL per 1 mmol Fmoc-aa). Protected amino acids (5-fold excess) were preactivated with HBTU/HOBt/DIPEA (5/5/10 equiv.) in DMF/NMP (8:2) at rt for 5 min and added to the resin. The vessel was shaken at rt or 35 °C for 60 min. The

coupling procedure was repeated ('double coupling'). After completed coupling of an Fmoc-aa, the resin was washed with DMF/NMP (8:2) (4×) followed by Fmoc deprotection with 20% piperidine in DMF/NMP (8:2) at rt (2 × 10 min) and washing of the resin with DMF/NMP (8:2) (5×). After coupling and Fmoc-deprotection of the final Fmoc-aa, a mixture formed by acetic anhydride (5 equiv.) and DIPEA (10 equiv.) in DMF/NMP (8:2) was added and the vessel was shaken at rt for 30 min followed by washing with DMF/NMP (8:2) (4×) and CH_2Cl_2 (treated with K_2CO_3) (6×). The side-chain protected peptides were cleaved off by treatment of the resin with CH_2Cl_2/HFIP (4:1 v/v) at rt (2 × 20 min). The resin was separated by filtration and washed once with CH_2Cl_2/HFIP (4:1) (ca 1 mL). The filtrates were combined, the volatiles evaporated and the residue was dissolved in acetonitrile/water (2:8 or 3:7 v/v) (ca 2 mL) followed by the addition of water (ca 50 mL) and lyophilization. Compounds **11-25** were used in the next step without purification. The chemical identities and purities of **11-25** were assessed by HRMS and analytical HPLC (data not shown).

General procedure for the synthesis of compounds 28-53. The coupling of the side chain-protected peptides **11-25** to amines **26** or **27** was performed in 1.5- or 2-mL polypropylene reaction vessels with screw cap. HOBt (1.2 equiv.) and EDC (1.2 equiv.) were added to a cooled (5 °C) solution of the respective side chain-protected peptide (1 equiv.) in DMF (0.1-0.4 mL). In the case of compounds derived from **26**, a solution of **26** (tetrakis(hydrotrifluoroacetate), 1-1.2 equiv.) and DIPEA (3 equiv.) in DMF (0.1 mL) was immediately added and stirring was continued at 5 °C for 3 h. For the synthesis of compounds derived from **27** a solution of **27** (free base, 1-1.2 equiv.) in DMF (0.1 mL) was immediately added and stirring was continued at 5 °C for 3 h. 1% aq TFA (0.1-0.4 mL, depending on the amount of DMF used to dissolve the peptide) was added and the mixture was subjected to preparative HPLC to isolate the protected intermediates (conditions not given). The latter were dissolved in TFA/CH_2Cl_2/H_2O (10:10:1 v/v/v) (products without Arg) or TFA/H_2O

(95:5 v/v) (products containing Arg). The mixtures were stirred at rt for 3 h, CH_2Cl_2 (ca 20 mL) was added and the volatiles were removed by evaporation. The final products were purified by preparative HPLC.

Experimental synthetic protocols and analytical data of compounds 55, 56 and 58. (*S*)-2-Amino-5-guanidino-*N*-(4-(1-(2-oxo-2-(11-oxo-10,11-dihydro-5*H*-dibenzo[*b*,*e*][1,4]diazepin-5-yl)ethyl)piperidin-4-yl)butyl)pentanamide tris(hydrotrifluoroacetate) (55) Compound **55** was prepared from amine **27** (55.6 mg, 0.137 mmol) and compound **54** (60 mg, 0.114 mmol) according to the general procedure for the synthesis of **28-53**. Purification by preparative HPLC (gradient: 0-25 min: 0.1% aq TFA/acetonitrile 81:19-72:28, t_R = 7 min) yielded **55** as a white fluffy solid (67 mg, 0.074 mmol, 65%). Ratio of configurational isomers evident in the NMR spectra: ca 1.5:1. ^{1}H-NMR (600 MHz, DMSO-d_6): δ (ppm) 1.13-1.29 (m, 4H), 1.30-1.52 (m, 7H), 1.64-1.71 (m, 2H), 1.71-1.83 (m, 2H), 2.83-2.96 (m, 1H), 2.96-3.04 (m, 1H), 3.04-3.14 (m, 4H), 3.28-3.35 (m, 0.8H), 3.55-3-63 (m, 1.2H), 3.65-3.73 (m, 1H), 3.75 (d, 0.6H, *J* 17 Hz), 3.90 (d, 0.4H, *J* 17 Hz), 4.32-4.48 (m, 1H), 6.95-7.49 (m, 7H), 7.49-7.56 (m, 1.4H), 7.56-7.63 (m, 0.6H), 7.63-7.79 (m, 2H), 7.79-7.92 (m, 2H), 8.11-8.24 (m, 3H), 8.41-8.48 (m, 1H), 9.57 (brs, 1H), 10.73 (s, 0.4H), 10.78 (s, 0.6H). ^{13}C-NMR (150.9 MHz, MeOH-d_4): δ (ppm) 22.32, 24.20, 28.31, 28.74, 28.98, 32.81, 34.95, 38.67, 40.08, 51.94, 52.80, 53.24, 55.96, 116.05 (TFA), 118.04 (TFA), 121.91, 122.34, 124.93, 125.51, 126.75, 127.27, 127.71, 128.75, 129.00, 129.71, 130.04, 130.38, 130.97, 131.63, 133.07, 133.80, 134.68, 135.77, 140.99, 156.84, 158.3 (q, *J* 32 Hz, carbonyl group of TFA), 163.70, 164.35, 165.78, 166.07, 168.05, 171.50. HRMS (ESI): *m/z* $[M+H]^+$ calcd. for $[C_{30}H_{43}N_8O_3]^+$ 563.3453, found 563.3462. RP-HPLC (220 nm): 99% (t_R = 6.2 min, *k* =7.1). $C_{30}H_{42}N_8O_3 \cdot C_6H_3F_9O_6$ (562.72 + 342.07).

(*S*)-2-Acetamido-5-guanidino-*N*-(4-(1-(2-oxo-2-(11-oxo-10,11-dihydro-5*H*-dibenzo[*b,e*][1,4]diazepin-5-yl)ethyl)piperidin-4-yl)butyl)pentanamide bis(hydrotrifluoroacetate) (56) Acetyl anhydride (3.6 µL, 0.038 mmol) was added to a solution of **55** (25 mg, 0.032 mmol) and DIPEA (28 µL, 0.16 mmol) in DMF (0.3 mL) and the mixture was stirred at rt for 2 h. Isolation of the product by preparative HPLC (gradient: 0-25 min: 0.1% aq TFA/acetonitrile 81:19-72:28, t_R = 9 min) afforded **56** as a white fluffy solid (20.8 mg, 0.025 mmol, 78%). Ratio of configurational isomers evident in the NMR spectra: ca 1.5:1. ^{1}H-NMR (600 MHz, DMSO-d_6): δ (ppm) 1.13-1.26 (m, 4H), 1.30-1.50 (m, 8H), 1.57-1.66 (m, 1H), 1.69-1.82 (m, 2H), 1.83 (s, 3H), 2.85-2.96 (m, 1H), 2.96-3.14 (m, 5H), 3.28-3.35 (m, 1H), 3.57-3.61 (m, 1H), 3.76 (d, 0.6H, *J* 16 Hz), 3.91 (d, 0.4H, *J* 16 Hz), 4.13-4.21 (m, 1H), 4.33-4.48 (m, 1H), 7.03 (brs, 2H), 7.20-7.31 (m, 2H), 7.31-7.39 (m, 1.6H), 7.39-7.49 (m, 1.4H), 7.49-7.55 (m, 1.4H), 7.55-7.62 (m, 0.6H), 7.62-7.79 (m, 3H), 7.79-7.85 (m, 0.6H), 7.85-7.93 (m, 1.4H), 7.95-8.02 (m, 1H), 9.55 (brs, 1H), 10.73 (s, 0.4H), 10.78 (s, 0.6H). ^{13}C-NMR (150.9 MHz, MeOH-d_4): δ (ppm) 22.49, 25.16, 28.69, 29.09, 29.26, 32.74, 34.90, 38.31, 40.33, 52.13, 52.65, 52.78, 53.23, 55.93, 116.05 (TFA), 118.10 (TFA), 121.88, 122.30, 124.89, 125.47, 126.74, 127.25, 127.70, 128.25, 128.70, 128.95, 129.69, 130.00, 130.36, 131.61, 133.03, 133.76, 134.68, 135.77, 140.97, 156.77, 158.2 (broad signal, carbonyl group of TFA), 163.67, 164.17, 165.73, 166.03, 169.19, 171.22. HRMS (ESI): *m/z* $[M+H]^+$ calcd. for $[C_{32}H_{45}N_8O_4]^+$ 605.3558, found 605.3560. RP-HPLC (220 nm): 98% (t_R = 8.0 min, *k* = 9.5). $C_{32}H_{44}N_8O_4 \cdot C_4H_2F_6O_4$ (604.76 + 228.05).

***N*-(4-(1-(2-Oxo-2-(11-oxo-10,11-dihydro-5*H*-dibenzo[*b,e*][1,4]diazepin-5-yl)ethyl)piperidin-4-yl)butyl)propionamide hydrotrifluoroacetate (58)** DIPEA (12 µL, 0.071 mmol) and a solution of **57** (12 mg, 0.071 mmol) in DMF (30 µL) were added to a solution of **27** (28 mg, 0.071 mmol) in DMF (0.25 mL) and the mixture was stirred at rt for 30 min followed by the addition of 10% aq TFA (0.14 mL). Purification by preparative HPLC

(gradient: 0-30 min: 0.1% aq TFA/acetonitrile 90:10-57:43, t_R = 18 min) yielded **58** as a white fluffy solid (33 mg, 0.057 mmol, 80%). Ratio of configurational isomers evident in the NMR spectra: ca 1.5:1. ^{1}H-NMR (600 MHz, MeOH-d_4): δ (ppm) 1.11 (t, 3H, *J* 7.7 Hz), 1.27-1.37 (m, 4H), 1.38-1.56 (m, 5H), 1.85-2.00 (m, 2H), 2.17 (q, 2H, *J* 7.7 Hz), 2.87-2.96 (m, 1H), 2.99-3.08 (m, 1H), 3.15 (t, 2H, *J* 7.1 Hz), 3.39-3.49 (m, 1H), 3.67-3.83 (m, 2H), 4.39 (d, 0.6H, *J* 17 Hz), 4.43 (d, 0.4H, *J* 17 Hz), 7.23-7.31 (m, 0.8H), 7.31-7.36 (m, 1.2H), 7.36-7.41 (m, 0.4H), 7.44-7.55 (m, 2.2H), 7.59-7.71 (m, 2H), 7.73-7.78 (m, 0.4H), 7.90 (d, 0.6H, *J* 8.1 Hz), 7.97 (d, 0.4H, *J* 7.8 Hz). ^{13}C-NMR (150.9 MHz, MeOH-d_4): δ (ppm) 10.59, 24.66, 30.22, 30.41, 30.47, 34.39, 36.31, 40.07, 54.95, 55.01, 55.37, 57.94, 58.04, 123.08, 123.64, 126.84, 127.51, 127.87, 128.49, 128.89, 129.45, 130.10, 130.54, 130.88, 131.20, 131.70, 131.97, 132.34, 133.01, 133.43, 134.57, 134.94, 135.45, 135.73, 137.04, 141.02, 142.68, 162.1 (broad signal, carbonyl group of TFA), 164.96, 165.45, 168.56, 168.81, 177.02. HRMS (ESI): *m/z* $[M+H]^+$ calcd. for $[C_{27}H_{35}N_4O_3]^+$ 463.2709, found 463.2729. RP-HPLC (220 nm): 99% (t_R = 8.3 min, *k* = 8.0). $C_{27}H_{34}N_4O_3 \cdot C_2HF_3O_2$ (462.59 + 114.02).

Cell culture. CHO-K9 cells, stably transfected with the DNA of human muscarinic receptors M_1-M_5 (obtained from Missouri S&T cDNA Resource Center; Rolla, MO) were cultured in HAM's F12 medium supplemented with fetal calf serum (Biochrom, Berlin, Germany) (10%) and G418 (Biochrom) (750 μg/mL). HEK-293 cells were maintained in DMEM/HAM's F12 (Thermo Scientific) supplemented with fetal bovine serum (Thermo Scientific) (10%) and Penicillin/Streptomycin (Thermo Scientific) (10,000 U/mL).

IP1 accumulation assay. The measurement of M_2R stimulated activation of the G-protein mediated pathway was performed as previously described applying the IP-One HTRF assay (Cisbio, Codolet, France) according to the manufacturer's protocol.[15] In brief, HEK-293 cells were grown to a confluency of approximately 70% and transiently cotransfected with the

cDNAs of the human M_2 receptor (Missouri S&T cDNA Rescourse Center) and the hybrid G-protein $G_{\alpha qi5\text{-}HA}$ ($G\alpha_q$ protein with the last five amino acids at the C-terminus replaced by the corresponding sequence of $G\alpha_i$; gift from the J. David Gladstone Institutes, San Francisco, CA),[19, 29] using TransIT-293 Mirus transfection reagent (MoBiTec, Goettingen, Germany). After 1 day, cells were detached from the culture dish with Versene (Life Technologies, Darmstadt, Germany), seeded into black 384-well plates (10,000 cells/well) (Greiner Bio-One, Frickenhausen, Germany) and maintained for 24 h at 37 °C. After incubation with the test compounds, dissolved in stimulation buffer, at 37 °C for 1 h the detection reagents were added (IP1-d2 conjugate and Anti IP1cryptate TB conjugate, each dissolved in lysis buffer), and incubation was continued at rt for 60 min. Time resolved fluorescence resonance energy transfer (HTRF) was determined using a Clariostar plate reader (BMG, Ortenberg, Germany) measuring fluorescence at 620 (±10) nm and 670 (±10) nm (excitation at 330 nm). Antagonistic activities of **38** and **48** were determined after preincubation of the cells with **38** or **48** for 30 min, followed by addition of CCh (final concentration: 0.3 μM) and continued incubation at 37 °C for 1 h.

Radioligand competition binding. Competition binding experiments with [^{3}H]NMS (specific activity: 80 Ci/mmol; purchased from American Radiolabeled Chemicals (St. Louis, MO) via Hartman Analytics (Braunschweig, Germany) were performed at intact CHO-hM_xR cells (x = 1-5) as described previously with minor modifications.[14] Cells were seeded in tissue culture treated white 96-well plates with clear bottom (Corning Incorporated Life Sciences, Tewksbury, MA; Corning cat. no. 3610) one or two days prior to the experiment. Depending on the level of receptor expression,[14] the confluency of the cells was 30–50% (M_1R), 50-70% (M_3R, M_4R, M_5R) or 90-100% (M_2R) on the day of the experiment. All experiments were performed at 22 ± 1 °C. The culture medium was removed by suction, the cells were washed with phosphate buffered saline (PBS) (200 μL) and covered with 160 μL of Leibovitz's L15

medium (Life Technologies) supplemented with 1% bovine serum albumin (Serva, Heidelberg, Germany), in the following referred to as L15 medium. For total binding L15 medium (20 µL) and L15 medium (20 µL) containing [^{3}H]NMS (10-fold concentrated) were added. To determine unspecific binding and the effect of a compound of interest on [^{3}H]NMS equilibrium binding, L15 medium (20 µL) containing atropine or the compound of interest (10-fold concentrated) and L15 medium (20 µL) containing [^{3}H]NMS (10-fold concentrated) were added. Samples were incubated for 3 h under gentle shaking. After incubation, the liquid was removed by suction, the cells were washed twice with ice-cold PBS (200 µL) and lysis solution (urea (8 M), acetic acid (3 M) and Triton-X-100 (1%) in water) (25 µL) was added. The plates were shaken for 30 min, liquid scintillator (Optiphase Supermix, PerkinElmer, Rodgau, Germany) (200 µL) was added, and the plates were sealed with a transparent sealing tape (permanent seal for microplates, PerkinElmer, prod. no. 1450–461). The plates were turned up-side down several times in order to achieve complete mixing of scintillator and lysis solution. The samples were kept in the dark for at least 1 h prior to the measurement of radioactivity (dpm) with a MicroBeta2 plate counter (PerkinElmer). Applied concentrations of [^{3}H]NMS: 0.2 nM (M_1R, M_2R, M_3R), 0.1 nM (M_4R), 0.3 nM (M_5R) or 2 nM (M_2R). Unspecific binding was determined in the presence of atropine (1000-fold excess to [^{3}H]NMS) and amounted to < 15% of total binding.

Investigation of the stability of 38, 48 and 52 in human plasma. The metabolic stabilities of **38**, **48** and **52** were investigated in human blood plasma/PBS pH 7.4 (1:2 v/v) (in the following referred to as plasma/PBS) at 37 °C. 1-Methyl-D-tryptophan (**59**) was used as internal standard. As the purity (RP-HPLC, 220 nm) of **59** was < 95% (data not shown) it was purified by preparative HPLC to give a purity of > 99%. Plasma was obtained by the collection of human blood from a healthy donor in 5.5-mL heparinized plasma-monovettes, followed by centrifugation at 1200 g at 4 °C for 10 min. The supernatants were pooled in two

50-mL Falcon tubes and centrifuged again at 1200 g at 4 °C for 10 min. The plasma was aliquoted and stored at −80 °C.

For the addition of the compounds to plasma/PBS, 5 mM stock solutions in acetonitrile/0.04% aqueous TFA (3:7 v/v) were used. Recoveries were determined for concentrations of 80 μM and 4 μM, and an internal standard concentration of 10 μM. For this purpose, **59** and the DIBA-peptide conjugates were added to plasma/PBS (total volume: 70 μL), immediately followed by vortexing (ca 10 s) and precipitation of protein by the addition of EtOH/acetonitrile (1:1 v/v) (140 μL). The mixture was vortexed for 5 min und centrifuged at 16,100 g at 4 °C for 10 min. Aliquots (180 μL) of the supernatant were transferred into 1.5-mL polypropylene reaction vessels containing 10% aqueous TFA (5 μL). The volatiles were removed in a vacuum concentrator under reduced pressure at 40 °C (ca 60 min), and the residue was taken up in acetonitrile/0.04% aqueous TFA (1:9 v/v) (90 μL) by vortexing (2 min). The samples were filtrated using a 0.2-μm RC-membrane filter (Phenomenex, Aschaffenburg, Germany) and analyzed by RP-HPLC using the analytical HPLC system and the conditions as described under general experimental conditions, but applying the following gradient: 0–12 min: A/B 90:10–70:30, 12–16 min: 70:30–5:95, 16–20 min: 5:95. On the day of an experiment four-point calibrations were performed for the respective DIBA-peptide conjugates and the internal standard. Peak areas representing 100% recovery were obtained by analyzing 53.3 μM and 2.67 μM DIBA-peptide solutions as well as a 6.67 μM solution of **59** (in duplicate each). All peak areas were transformed into concentrations (μM) and percent recoveries of **38**, **48**, **52** and **59** were calculated based on the average values of the 100% reference samples (see Table S2, Supporting Information). Recovery ratios were obtained by dividing the recovery of the DIBA-peptide conjugate by the recovery of **59** for each individual sample (n = 3 or 4, *cf.* Table S2, Supporting Information).

For the investigation of the stabilities in plasma, the DIBA-peptide conjugates (**38**, **48**, **52**) and **59** were added to plasma/PBS at a concentration of 100 μM and 10 μM, respectively (in

triplicate each). After 1, 6, 24 and 48 h of incubation under shaking at 37 °C, aliquots (70 µL) were taken and processed as described above for the determination of recoveries. On the day of an experiment four-point calibrations were performed for the respective DIBA-peptide conjugates and **59**. Peak areas representing 100% recovery were obtained by analyzing 66.7 µM 'DIBA-peptide' solutions and a 6.67 µM solution of **59** (in duplicate). Based on the calibration, the peak areas of the 100% references and of the samples were transformed into concentrations (µM). Recoveries of **38**, **48** and **52** were calculated by multiplying the recovery of **59**, obtained for each individual sample, with the recovery ratio obtained for the concentration of 80 µM (see above). The plasma concentrations of the DIBA-peptide conjugates were obtained by dividing the determined 'DIBA-peptide' concentration by the respective recovery. Degradation (%) of **38**, **48** and **52** was calculated based on the average values of the 100% reference samples.

Note: recovery ratios obtained for a concentration of 4 µM were not used as **38**, **48** and **52** exhibited high stabilities (lowest concentration in plasma ca 80 µM (**52**, 48 h)).

Molecular dynamics simulations

MR models. In case of the hM_2R, a described model derived from the M_2R crystal structure (PDB ID: 3UON[21]) was used.[15] Models of the hM_1R, hM_3R and hM_4R were obtained by refinement of reported crystal structures (PDB ID 5CXV,[3] PDB ID 4DAJ[22] and PDB ID 5DSG,[3] respectively) using Modeller 9.18[30-32] The homology model of the hM_5R was prepared based on the M_2R crystal structure (PDB ID: 3UON[21]) using Modeller 9.18. Replacement of ICL3 of the hM_1R, hM_3R, hM_4R and hM_5R by eight alanines was performed using the respective coordinates of the described hM_2R model.[15] The receptor models (M_1R, M_2R, M_3R, M_4R, M_5R) contained a disulfide bridge between $Cys^{3.25}$ and $Cys^{ECL2.50}$ as well as between the two cysteines in ECL3. Coordinates other than ligand and receptor molecules were removed. The protein preparation wizard (Schrödinger LLC, Portland, OR USA) was

used to further refine the receptor models: The N- and C-termini were capped by the introduction of acetyl and methylamide groups, respectively, and amino acid side chains containing hydrogen bond donors and acceptors were optimized for hydrogen bonding. Histidine residues were simulated in the uncharged form as the N^{ε}–H tautomer. Residues other than histidine were simulated in their dominant protonation state at pH 7. The above mentioned disulfide bonds were maintained and a sodium ion was placed next to $D^{2.50}$.[33]

Induced-fit docking. For induced-fit docking, performed to find the initial ligand binding poses for MD simulations, ligand (**38**, **48**) geometries were energetically optimized using the LigPrep module (Schrödinger LLC). Amine (piperidine, piperazine (singly protonated), Lys) and guanidine (Arg) groups in **38** and **48** were protonated resulting in net charges of +4 and +3, respectively. For initial docking, two strategies were pursued: either $Y^{3.33}$, $Y^{6.51}$ and $Y^{7.39}$ were temporarily mutated to alanine (Gridgen_Recep_Vscale = 0.7) or mutations were omitted (Gridgen_Recep_Vscale = 0.5). Ligands were docked within a box of 46 × 46 × 46 $Å^3$ around the crystallographic binding poses of the co-crystallized ligands. Redocking was performed in the extended precision mode. From the obtained induced-fit docking results of each MR subtype/ligand combination, one pose (ligand-receptor complex) was selected as input structure for the MD simulation based on low/minimal MM-GBSA scores (Schrödinger LLC, implicit membrane model) and reasonability of the ligand binding pose.

MD simulations. The selected ligand-receptor complexes were aligned to the aforementioned crystal structure entries in the orientations of proteins in membranes (OPM) database[34] using the protein structure alignment tool (Schrödinger LLC). Ligand-receptor complexes were inserted into a hydrated palmitoyloleoylphosphatidylcholine (POPC) bilayer (comprising 160 POPC molecules) as described for **7**.[15] The systems contained about 61,000-68,000 atoms and the initial box sizes were approximately 82 × 82 × (99-110) $Å^3$. The parameters (geometry, partial charges) of the protein structure, ligands (**38**, **48**), lipids, inorganic ions, and water were assigned as reported.[15] MD simulations were executed on Nvidia GTX 1080(Ti) GPUs

using the CUDA version of PMEMD,[35, 36] implemented in AMBER18 (AMBER 2018, University of California, San Francisco, CA USA). After minimization, the systems were heated from 0 to 100 K in the NVT ensemble during 20 ps and from 100 to 310 K in the NPT ensemble during 100 ps, applying harmonic restraints of 5 kcal · mol^{-1} · $Å^{-1}$ to non-hydrogen atoms of protein, lipids and ligand. The temperature and pressure coupling parameters used for the equilibration at 310 K (NPT ensemble) were the same as described for MD simulations of the hM_2R bound to **7**.[15] During the 10 ns equilibration period, harmonic restraints on receptor and ligand non-hydrogen atoms were reduced stepwise (0.5 kcal · mol^{-1} · $Å^{-1}$ every 0.5 ns) to 2.5 kcal · mol^{-1} · $Å^{-1}$ within 3 ns. While removing restraints on ligand atoms, harmonic restrains on receptor mainchain atoms were further reduced stepwise (0.5 kcal · mol^{-1} · $Å^{-1}$ every 0.5 ns) to 0.5 kcal · mol^{-1} · $Å^{-1}$ from 3 to 5 ns. After 5 ns, harmonic restraints on receptor mainchain atoms were removed, i.e. the residual equilibration period (5 ns) was run without restraints. The interaction cutoff was set to 9.0 Å, and long-range electrostatics were computed using the particle mesh Ewald (PME) method.[37] To enable a frame step size of 4 fs, bonds involving hydrogen atoms were constrained using SHAKE[38] and hydrogen mass repartitioning (HMR)[39] was applied. The final frame of the equilibration period was used as input for the simulations over 20.25 µs. After the equilibration period of 10 ns, the Berendsen Barostat was replaced by the Monte Carlo Barostat algorithm.[40]

Data were collected every 500 ps. For analyses, the first 250 ns of the simulations were omitted and every twentieth frame (10 ns step size) was considered. To determine the frame corresponding to the lowest binding free energy, MM-PBSA calculations of the MD simulation (20 µs) trajectories were performed using AMBER18. Ligand-receptor interactions were analyzed using PLIP 1.4.2.[41] For time course illustrations, frames were collected every 1 µs (20 frames). Figures showing molecular structures (Figure 4, Figures S8-S15) were generated with PyMOL Molecular Graphics system, version 2.2.0 (Schrödinger LLC).

Data processing. Specific optical rotations were calculated according to $[\alpha]_D^{20} = \alpha/(c \cdot l)$ (α = measured angle of rotation [deg], c = concentration [g cm^{-3}], l = length of the cuvette [dm]). Retention (capacity) factors were calculated from retention times (t_R) according to $k = (t_R - t_0)/t_0$ (t_0 = dead time). Data from radioligand ([^{3}H]NMS) competition binding assays (except for **48**, M_3R) and from the IP1 accumulation assay were processed as reported previously, but pIC_{50} values obtained from the IP1 assay (antagonist mode) were not converted to pK_b values.[15] In case of competition binding studies with [^{3}H]NMS and **48** at the M_3R, pIC_{50} values were obtained from a linear Hill plot ($\log(B/(B_0 - B)$ plotted against log(concentration of **48**); B = specifically bound [^{3}H]NMS in the presence of **48**, B_0 = specifically bound [^{3}H]NMS in the absence of **48**; log(concentration of **48**) at '$\log(B/(B_0 - B) = 0$' equals the pIC_{50}). K_i values for the calculation of relative MR affinities (M_2R selectivity, Table 1) were obtained by transforming pIC_{50} values from individual competition binding experiments with [^{3}H]NMS to IC_{50} values followed by conversion to K_i values according to the Cheng-Prusoff equation[42] and calculation of mean K_i values.

AUTHOR INFORMATION

Corresponding Author

*E-mail: max.keller@ur.de. Phone: (+49)941-9433329. Fax: (+49)941-9434820

Present Addresses

[‖]Ramboll Environment & Health GmbH, Werinherstraße 79, D-81541 Munich, Germany

[§]Moffitt Cancer Center, 12902 USF Magnolia Drive, Tampa, FL, USA

Author Contributions

[#]These authors contributed equally.

A.P., C.G.G., M.K. and X.S. performed the syntheses and the analytical characterization of chemical compounds. A.P., C.G.G. and M.K. performed radioligand competition binding experiments and analyzed the data. H.H. and P.G. performed IP1 accumulation assays and analyzed the data. C.G.G. investigated plasma stabilities. D.W. performed molecular docking and MD simulations and processed the data. D.W., A.P. and M.K. designed the MR ligands. M.K. initiated and planned the project. M.K. and G.B. supervised the research. M.K., A.P., D.W., G.B. and C.G.G. wrote the manuscript. All authors have given approval to the final version of the manuscript.

Funding Sources

This work was funded by the Graduate Training Program (Graduiertenkolleg) GRK1910 of the Deutsche Forschungsgemeinschaft and by the China Scholarship Council.

Notes

The authors declare no competing financial interest.

ACKNOWLEDGMENT

The authors thank Susanne Bollwein, Brigitte Wenzl, Lisa Schindler and Maria Beer-Krön for excellent technical assistance, Armin Buschauer for providing laboratory equipment and for helpful discussions as well as the Leibniz Rechenzentrum (LRZ) in Munich for providing software (Schrödinger Suite) and computing resources.

ABBREVIATIONS

CCh, carbachol; CHO-cells, Chinese hamster ovary cells; DIPEA, diisopropylethylamine; EDC, *N*-(3-dimethylaminopropyl)-*N*′-ethylcarbodiimide hydrochloride; GPCR, G-protein coupled receptor; HBTU, *O*-(1*H*-benzotriazol-1-yl)-*N*,*N*,*N*′,*N*′-tetramethyluronium

hexafluorophosphate; HFIP, 1,1,1,3,3,3-hexafluoro-2-propanol; HOBt, 1-hydroxybenzotriazole hydrate; HRMS, high resolution mass spectrometry, IP1, inositol monophosphate; *k*, retention (or capacity) factor (HPLC); K_d, dissociation constant obtained from a saturation binding experiment; K_i, dissociation constant obtained from a competition binding experiment; MR, muscarinic receptor; M_xR, muscarinic receptor subtype x; NMS, N-methylscopolamine; PBS, phosphate buffered saline; PS, polystyrene, TFA, trifluoroacetic acid; t_R, retention time.

ASSOCIATED CONTENT

The Supporting Information is available free of charge on the ACS Publications website at DOI:

Analytical data of compounds **28-53**; Figures S1-S8; MD simulations with the M_1R, M_2R, M_4R and M_5R bound to **38** and with the M_1R-M_5R bound to **48** (Figures S9-S15); Tables S1 and S2; RP-HPLC chromatograms of **28-53**, **55**, **56** and **58**; ^{1}H- and ^{13}C-NMR spectra of compounds **28-53**, **55**, **56** and **58** (PDF).

Molecular formula strings (CSV).

Coordinates of the homology model of the hM_5R, which was prepared based on a reported crystal structure of the M_2R (PDB ID: 3UON[21]) (PDB). Authors will release the atomic coordinates upon article publication.

REFERENCES

(1) Eglen, R. M. Overview of muscarinic receptor subtypes. *Handb. Exp. Pharmacol.* **2012,** *208*, 3-28.

(2) Gregory, K. J.; Sexton, P. M.; Christopoulos, A. Allosteric modulation of muscarinic acetylcholine receptors. *Curr. Neuropharmacol.* **2007,** *5*, 157-167.

(3) Thal, D. M.; Sun, B.; Feng, D.; Nawaratne, V.; Leach, K.; Felder, C. C.; Bures, M. G.; Evans, D. A.; Weis, W. I.; Bachhawat, P.; Kobilka, T. S.; Sexton, P. M.; Kobilka, B. K.; Christopoulos, A. Crystal structures of the M_1 and M_4 muscarinic acetylcholine receptors. *Nature* **2016,** *531*, 335-340.

(4) Eglen, R. M.; Choppin, A.; Watson, N. Therapeutic opportunities from muscarinic receptor research. *Trends Pharmacol. Sci.* **2001,** *22*, 409-414.

(5) Sheardown, M. J. Muscarinic M_1 receptor agonists and M_2 receptor antagonists as therapeutic targets in Alzheimer's disease. *Expert Opin. Ther. Pat.* **2002,** *12*, 863-870.

(6) Clader, J. W.; Wang, Y. Muscarinic receptor agonists and antagonists in the treatment of Alzheimer's disease. *Curr. Pharm. Des.* **2005,** *11*, 3353-3361.

(7) Citron, M. Alzheimer's disease: strategies for disease modification. *Nat. Rev. Drug Discovery* **2010,** *9*, 387-398.

(8) Clader, J. W.; Billard, W.; Binch, H., 3rd; Chen, L. Y.; Crosby, G., Jr.; Duffy, R. A.; Ford, J.; Kozlowski, J. A.; Lachowicz, J. E.; Li, S.; Liu, C.; McCombie, S. W.; Vice, S.; Zhou, G.; Greenlee, W. J. Muscarinic M_2 antagonists: anthranilamide derivatives with exceptional selectivity and in vivo activity. *Bioorg. Med. Chem.* **2004,** *12*, 319-326.

(9) Dörje, F.; Wess, J.; Lambrecht, G.; Tacke, R.; Mutschler, E.; Brann, M. Antagonist binding profiles of five cloned human muscarinic receptor subtypes. *J. Pharmacol. Exp. Ther.* **1991,** *256*, 727-733.

(10) Doods, H. N.; Quirion, R.; Mihm, G.; Engel, W.; Rudolf, K.; Entzeroth, M.; Schiavi, G. B.; Ladinsky, H.; Bechtel, W. D.; Ensinger, H. A.; Mendla, K. D.; Eberlein, W. Therapeutic potential of CNS-active M_2 antagonists: novel structures and pharmacology. *Life Sci.* **1993,** *52*, 497-503.

(11) Doods, H.; Entzeroth, M.; Ziegler, H.; Schiavi, G.; Engel, W.; Mihm, G.; Rudolf, K.; Eberlein, W. Characterization of BIBN 99: a lipophilic and selective muscarinic M_2 receptor antagonist. *Eur. J. Pharmacol.* **1993,** *242*, 23-30.

(12) Maggio, R.; Barbier, P.; Bolognesi, M. L.; Minarini, A.; Tedeschi, D.; Melchiorre, C. Binding profile of the selective muscarinic receptor antagonist tripitramine. *Eur. J. Pharmacol.* **1994,** *268*, 459-462.

(13) Gitler, M. S.; Reba, R. C.; Cohen, V. I.; Rzeszotarski, W. J.; Baumgold, J. A novel m2-selective muscarinic antagonist: binding characteristics and autoradiographic distribution in rat brain. *Brain Res.* **1992,** *582*, 253-260.

(14) Keller, M.; Tränkle, C.; She, X.; Pegoli, A.; Bernhardt, G.; Buschauer, A.; Read, R. W. M_2 Subtype preferring dibenzodiazepinone-type muscarinic receptor ligands: Effect of chemical homo-dimerization on orthosteric (and allosteric?) binding. *Bioorg. Med. Chem.* **2015,** *23*, 3970-3990.

(15) Pegoli, A.; She, X.; Wifling, D.; Hübner, H.; Bernhardt, G.; Gmeiner, P.; Keller, M. Radiolabeled dibenzodiazepinone-type antagonists give evidence of dualsteric binding at the M_2 muscarinic acetylcholine receptor. *J. Med. Chem.* **2017,** *60*, 3314-3334.

(16) She, X.; Pegoli, A.; Mayr, J.; Huebner, H.; Bernhardt, G.; Gmeiner, P.; Keller, M. Heterodimerization of dibenzodiazepinone-type muscarinic acetylcholine receptor ligands leads to increased M_2R affinity and selectivity. *ACS Omega* **2017,** *2*, 6741-6754.

(17) De Amici, M.; Dallanoce, C.; Holzgrabe, U.; Trankle, C.; Mohr, K. Allosteric ligands for G protein-coupled receptors: a novel strategy with attractive therapeutic opportunities. *Med. Res. Rev.* **2010,** *30*, 463-549.

(18) Valant, C.; Robert Lane, J.; Sexton, P. M.; Christopoulos, A. The best of both worlds? Bitopic orthosteric/allosteric ligands of g protein-coupled receptors. *Annu. Rev. Pharmacol. Toxicol.* **2012,** *52*, 153-178.

(19) Kruse, A. C.; Ring, A. M.; Manglik, A.; Hu, J.; Hu, K.; Eitel, K.; Hübner, H.; Pardon, E.; Valant, C.; Sexton, P. M. Activation and allosteric modulation of a muscarinic acetylcholine receptor. *Nature* **2013,** *504*, 101-106.

(20) Christopoulos, A. Advances in G protein-coupled receptor allostery: from function to structure. *Mol. Pharmacol.* **2014,** *86*, 463-478.

(21) Haga, K.; Kruse, A. C.; Asada, H.; Yurugi-Kobayashi, T.; Shiroishi, M.; Zhang, C.; Weis, W. I.; Okada, T.; Kobilka, B. K.; Haga, T.; Kobayashi, T. Structure of the human M_2 muscarinic acetylcholine receptor bound to an antagonist. *Nature* **2012,** *482*, 547-551.

(22) Kruse, A. C.; Hu, J.; Pan, A. C.; Arlow, D. H.; Rosenbaum, D. M.; Rosemond, E.; Green, H. F.; Liu, T.; Chae, P. S.; Dror, R. O.; Shaw, D. E.; Weis, W. I.; Wess, J.; Kobilka, B. K. Structure and dynamics of the M_3 muscarinic acetylcholine receptor. *Nature* **2012,** *482*, 552-556.

(23) Dror, R. O.; Green, H. F.; Valant, C.; Borhani, D. W.; Valcourt, J. R.; Pan, A. C.; Arlow, D. H.; Canals, M.; Lane, J. R.; Rahmani, R.; Baell, J. B.; Sexton, P. M.; Christopoulos, A.; Shaw, D. E. Structural basis for modulation of a G-protein-coupled receptor by allosteric drugs. *Nature* **2013,** *503*, 295-299.

(24) Fish, I.; Stossel, A.; Eitel, K.; Valant, C.; Albold, S.; Huebner, H.; Moller, D.; Clark, M. J.; Sunahara, R. K.; Christopoulos, A.; Shoichet, B. K.; Gmeiner, P. Structure-based design and discovery of new M_2 receptor agonists. *J. Med. Chem.* **2017,** *60*, 9239-9250.

(25) Liu, H.; Hofmann, J.; Fish, I.; Schaake, B.; Eitel, K.; Bartuschat, A.; Kaindl, J.; Rampp, H.; Banerjee, A.; Hubner, H.; Clark, M. J.; Vincent, S. G.; Fisher, J. T.; Heinrich, M. R.; Hirata, K.; Liu, X.; Sunahara, R. K.; Shoichet, B. K.; Kobilka, B. K.; Gmeiner, P. Structure-guided development of selective M_3 muscarinic acetylcholine receptor antagonists. *Proc. Natl. Acad. Sci. U. S. A.* **2018,** *115*, 12046-12050.

(26) Suno, R.; Lee, S.; Maeda, S.; Yasuda, S.; Yamashita, K.; Hirata, K.; Horita, S.; Tawaramoto, M. S.; Tsujimoto, H.; Murata, T.; Kinoshita, M.; Yamamoto, M.; Kobilka, B. K.; Vaidehi, N.; Iwata, S.; Kobayashi, T. Structural insights into the subtype-

selective antagonist binding to the M_2 muscarinic receptor. *Nat. Chem. Biol.* **2018,** *14*, 1150-1158.

(27) Keller, M.; Pop, N.; Hutzler, C.; Beck-Sickinger, A. G.; Bernhardt, G.; Buschauer, A. Guanidine-acylguanidine bioisosteric approach in the design of radioligands: synthesis of a tritium-labeled N(G)-propionylargininamide ([^{3}H]-UR-MK114) as a highly potent and selective neuropeptide Y Y_1 receptor antagonist. *J. Med. Chem.* **2008,** *51*, 8168-8172.

(28) Aldrich, C.; Bertozzi, C.; Georg, G. I.; Kiessling, L.; Lindsley, C.; Liotta, D.; Merz, K. M., Jr.; Schepartz, A.; Wang, S. The ecstasy and agony of assay interference compounds. *J. Med. Chem.* **2017,** *60*, 2165-2168.

(29) Conklin, B. R.; Farfel, Z.; Lustig, K. D.; Julius, D.; Bourne, H. R. Substitution of three amino acids switches receptor specificity of Gq alpha to that of Gi alpha. *Nature* **1993,** *363*, 274-276.

(30) Marti-Renom, M. A.; Stuart, A. C.; Fiser, A.; Sanchez, R.; Melo, F.; Sali, A. Comparative protein structure modeling of genes and genomes. *Annu. Rev. Biophys. Biomol. Struct.* **2000,** *29*, 291-325.

(31) Sali, A.; Blundell, T. L. Comparative protein modelling by satisfaction of spatial restraints. *J. Mol. Biol.* **1993,** *234*, 779-815.

(32) Fiser, A.; Do, R. K.; Sali, A. Modeling of loops in protein structures. *Protein Sci.* **2000,** *9*, 1753-1773.

(33) Huang, W.; Manglik, A.; Venkatakrishnan, A. J.; Laeremans, T.; Feinberg, E. N.; Sanborn, A. L.; Kato, H. E.; Livingston, K. E.; Thorsen, T. S.; Kling, R. C.; Granier, S.; Gmeiner, P.; Husbands, S. M.; Traynor, J. R.; Weis, W. I.; Steyaert, J.; Dror, R. O.; Kobilka, B. K. Structural insights into micro-opioid receptor activation. *Nature* **2015,** *524*, 315-321.

(34) Lomize, M. A.; Lomize, A. L.; Pogozheva, I. D.; Mosberg, H. I. OPM: orientations of proteins in membranes database. *Bioinformatics* **2006,** *22*, 623-625.

(35) Salomon-Ferrer, R.; Gotz, A. W.; Poole, D.; Le Grand, S.; Walker, R. C. Routine microsecond molecular dynamics simulations with AMBER on GPUs. 2. explicit solvent particle mesh Ewald. *J. Chem. Theory Comput.* **2013,** *9*, 3878-3888.

(36) Le Grand, S.; Götz, A. W.; Walker, R. C. SPFP: Speed without compromise - a mixed precision model for GPU accelerated molecular dynamics simulations. *Comput. Phys. Commun.* **2013,** *184*, 374-380.

(37) Darden, T.; York, D.; Pedersen, L. Particle mesh Ewald: an N·log(N) method for Ewald sums in large systems. *J. Chem. Phys.* **1993,** *98*, 10089-10092.

(38) Ryckaert, J.-P.; Ciccotti, G.; Berendsen, H. J. C. Numerical integration of the cartesian equations of motion of a system with constraints: molecular dynamics of n-alkanes. *J. Comput. Phys.* **1977,** *23*, 327-341.

(39) Hopkins, C. W.; Le Grand, S.; Walker, R. C.; Roitberg, A. E. Long-time-step molecular dynamics through hydrogen mass repartitioning. *J. Chem. Theory Comput.* **2015,** *11*, 1864-1874.

(40) Chow, K.-H.; Ferguson, D. M. Isothermal-isobaric molecular dynamics simulations with Monte Carlo volume sampling. *Comput. Phys. Commun.* **1995,** *91*, 283-289.

(41) Salentin, S.; Schreiber, S.; Haupt, V. J.; Adasme, M. F.; Schroeder, M. PLIP: fully automated protein-ligand interaction profiler. *Nucleic Acids Res.* **2015,** *43*, W443-447.

(42) Cheng, Y.-C.; Prusoff, W. H. Relation between the inhibition constant (K_i) and the concentration of inhibitor which causes fifty per cent inhibition (IC_{50}) of an enzymic reaction. *Biochem. Pharmacol.* **1973,** *22*, 3099-3108.

Graphic for TOC

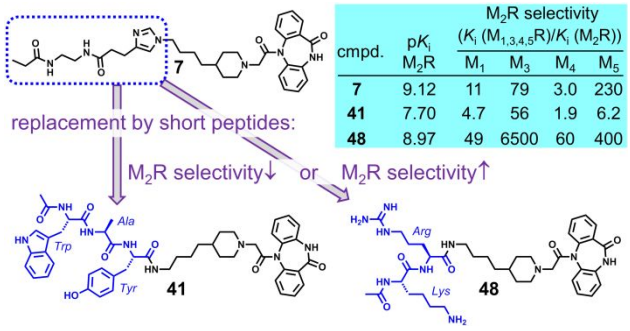

cmpd.	pK_i M_2R	M_2R selectivity (K_i ($M_{1,3,4,5}R$)/K_i (M_2R)) M_1	M_3	M_4	M_5
7	9.12	11	79	3.0	230
41	7.70	4.7	56	1.9	6.2
48	8.97	49	6500	60	400

Unable to Convert Image

The dimensions of this image (in pixels) are too large to be converted. For this image to convert, the total number of pixels (height x width) must be less than 40,000,000 (40 megapixels).

- preparation of 'DIBA-peptide conjugates':

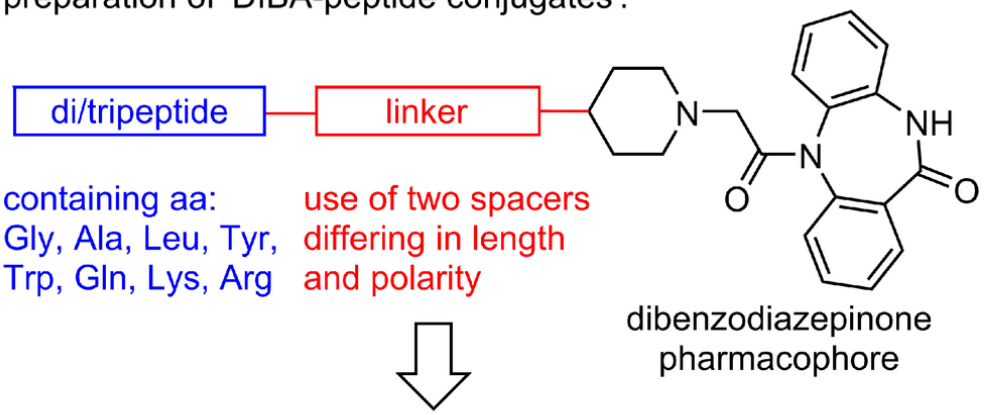

- determination of M_1-M_5 receptor binding data
- MD simulations of M_xRs (x = 1-5) bound to the most M_2R-selective compounds

83x48mm (300 x 300 DPI)

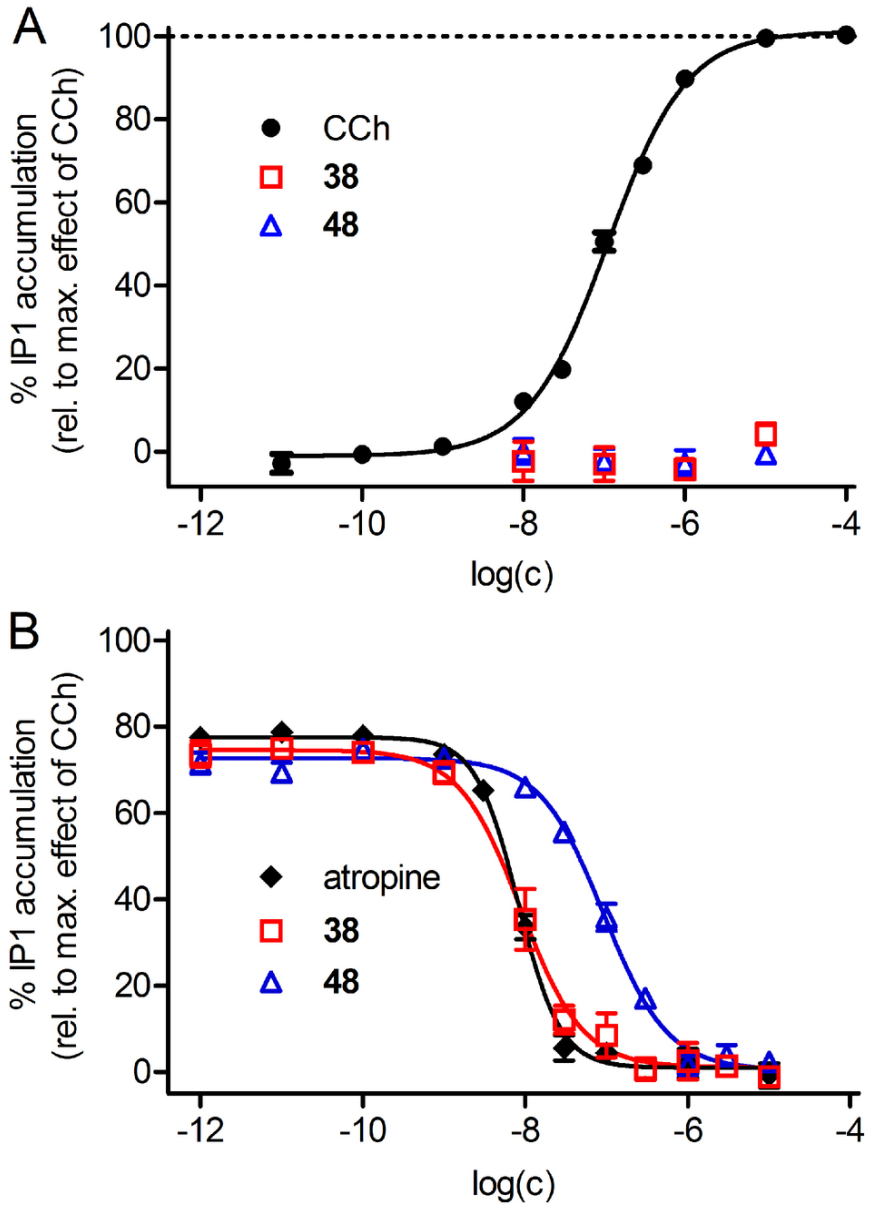

80x111mm (300 x 300 DPI)

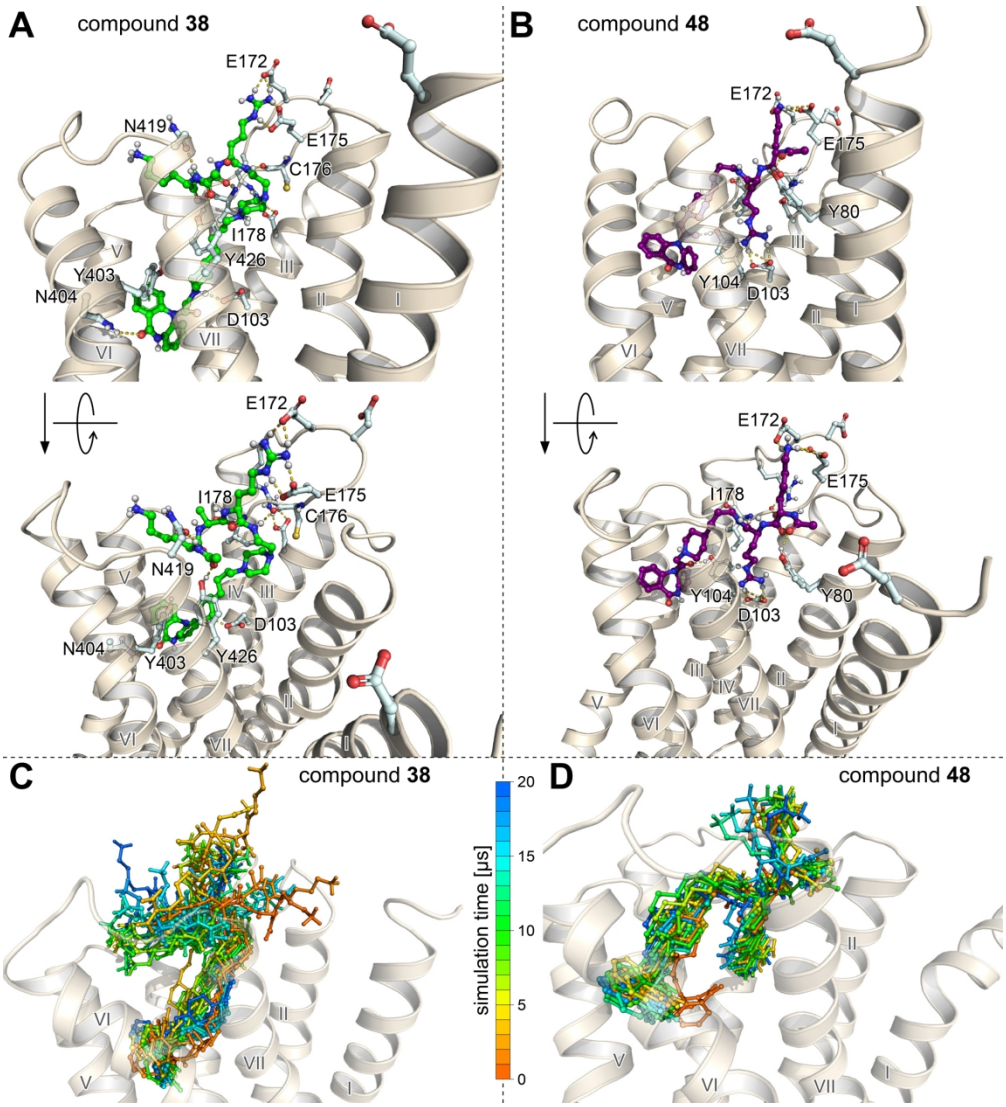
A
compound 38
E172
N419
E175
C176
I178
Y426
Y403
N404
D103
B
compound 48
E172
E175
Y80
Y104
D103
C
compound 38
D
compound 48
simulation time [µs]
20
15
10
5
0

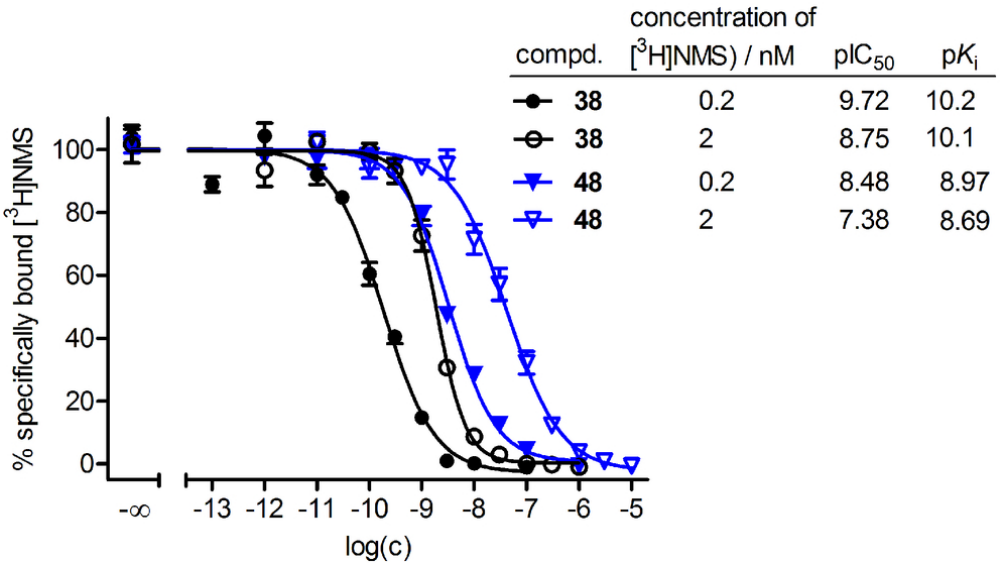

83x47mm (300 x 300 DPI)

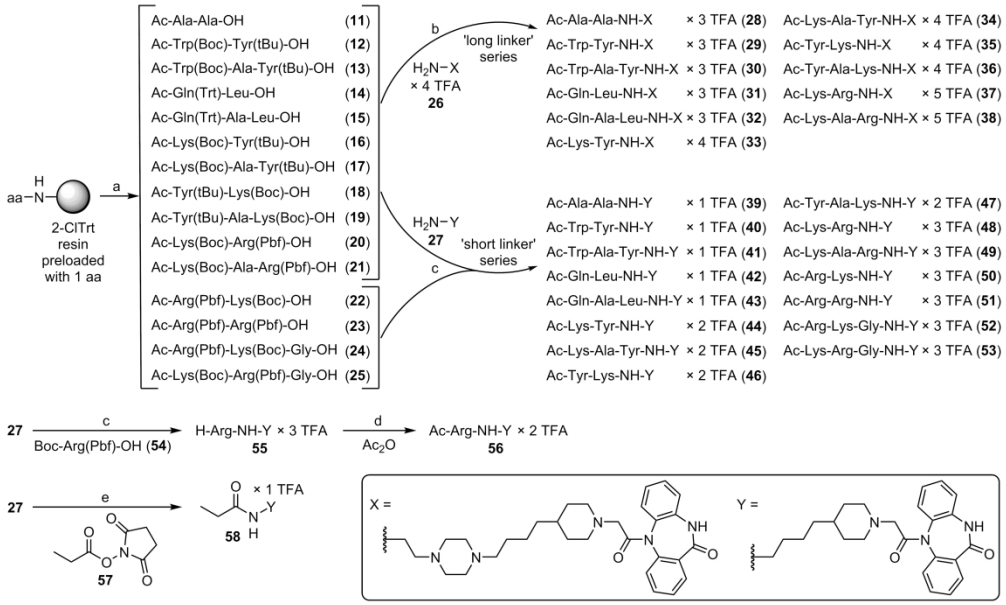

178x106mm (600 x 600 DPI)

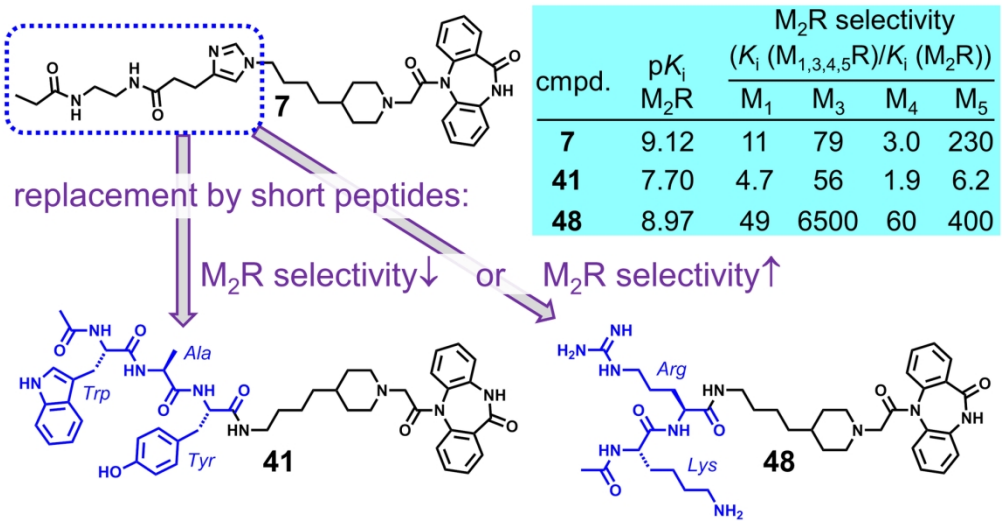

cmpd.	pK_i M_2R	M_2R selectivity (K_i ($M_{1,3,4,5}R$)/K_i (M_2R))			
		M_1	M_3	M_4	M_5
7	9.12	11	79	3.0	230
41	7.70	4.7	56	1.9	6.2
48	8.97	49	6500	60	400

82x42mm (600 x 600 DPI)